Sperotto, A.; Molina, J.; Torresan, S.; Critto, A.; Pulido-Velazquez, M.; Marcomini, A. (2019). A Bayesian Networks approach for the assessment of climate change impacts on nutrients loading. Environmental Science & Policy. 100:21-36. https://doi.org/10.1016/j.envsci.2019.06.004

# A Bayesian Networks approach for the assessment of climate change impacts on nutrients loading

Sperotto A.[1,2], Molina J.L.[3,] Torresan S.[1], Critto A.[1,2*], Pulido-Velazquez M.[4], Marcomini A. [1,2]

[1] Fondazione Centro Euro-Mediterraneo sui Cambiamenti Climatici (Fondazione CMCC), c/o via Augusto Imperatore 16, 73100 Lecce, Italy.

[2] Department of Environmental Sciences, Informatics and Statistics, University Ca' Foscari Venice, Via delle Industrie 21/8, I-30175 Marghera, Venezia, Italy.

[3] High Polytechnic School of Engineering, University of Salamanca, Av. de los Hornos Caleros, 50, 05003 Ávila, Spain.

[4] Research Institute of Water and Environmental Engineering and (IIAMA), Universitat Politècnica de València, Camino de Vera S/N – 46022 Valencia – Spain.

[*]Corresponding author: critto@unive.it

**Abstract**

Climate change is likely to strongly affect both the qualitative and quantitative characteristics of water resources. However, while potential impacts of climate change on water availability have been widely studied in the last decades, their implication for water quality have been just poorly explored since now. Accordingly, an integrated assessment based on Bayesian Networks (BNs) was implemented in the Zero river basin (Northern Italy) to capture interdependencies between future scenarios of climate change with water quality alterations (i.e. changes in nutrients loadings). Bayesian Networks were used as integrative tool for structuring and combining the information available in existing hydrological models, climate change projections, historical observations and expert opinion producing alternative risk scenarios to communicate the probability (and uncertainty) of changes in the amount nutrients (i.e. $NO_3^-$, $NH_4^+$, $PO_4^{3-}$) delivered from the basin under different climate change projections (i.e. RCP 4.5 and 8.5)

The model predictive accuracy and uncertainty were evaluated through a cross comparison with existing observed data and hydrological models' simulations (i.e. SWAT) available for the case study and, in addition, sensitivity analysis was performed to identify key input variables, knowledge gaps in model structurers and data. Simulated scenarios show that seasonal changes in precipitation and temperature are likely to modify both the hydrology and nutrient loadings of the Zero river with a high probability of an increase of freshwater discharge, runoff and nutrient loadings in autumn and a decrease in spring and summer with respect to the current conditions 1983-2012. Greater increase for both river flow and nutrients loadings are predicted under the medium and long term RCP8.5 scenarios. Diffuse pollution sources play a key role in determining the amount of nutrients loaded: both $NH_4^+$ and $PO_4^{3-}$ loadings are mainly influenced by changes in hydrological variables (i.e. runoff) while $NO_3^-$ loadings, despite being highly dependent on flow conditions, are also influenced by agronomic practices and land use (i.e. irrigation, fertilization). Highlighting key components and processes from a multi-disciplinary perspective, BN outputs could support water managers in tracking future trends of water quality and prioritizing stressors and pollution sources thus paving the way for the identification of targeted typologies of management and adaptation strategies to maintain good water quality status under climate change conditions.

**Introduction**

Climate change, in combination with other anthropogenic stressors (i.e. urbanization, agriculture, population growth), may affect the availability and quality of water in multiple ways (Jiménez Cisneros et al., 2014). However, while potential impacts of climate change on water availability have been widely studied in the last decades (Molina et al., 2013; Marcos-Garcia et al., 2017; Ronco et al., 2017; Zabel, 2016), their implication for water quality and their interaction with other drivers of change have been just poorly explored (Bussi et al., 2016; Huttunen et al., 2015; Lu et al., 2015; Pulido-Velazquez et al., 2015; Whitehead et al., 2008).

In Mediterranean climate regions, the high seasonal variability alternating dry and wet period is likely to have profound effects on those hydrological processes (e.g. runoff, river flow, water retention time, evapotranspiration) that regulate the mobilization of nutrients and other kinds of pollutants from land to water bodies (Alam and Dutta, 2013; Culbertson et al., 2016; El-Khoury et al., 2015; Ockenden et al., 2016). Likewise, increased temperature can accelerate the mineralization of organic matter in the soil (Eghball et al., 2002). Despite the fact that all these alterations are likely to affect nutrients availability and loadings, the magnitude, timing and seasonality of these changes are still largely unknown (Jiménez Cisneros et al., 2014).

A major challenge of understanding processes governing water quality under multiple stressors conditions is primarily represented by the need to combine and translate knowledge from many different disciplines and sources, into a single, logically consistent integrated framework. In fact, while some processes may be clearly described by deterministic or process-based models (e.g. hydrological models), other biophysical and socio-economic processes impacted by climatic and management changes are still not well understood, thus are inherently subjected to uncertainty. As a consequence, deterministic approaches relying solely on quantitative data, while having the advantage of providing a strong quantitative modelling of impacts, could not be useful when there is limited information about the effect of human decisions on the system. Moreover, when dealing with natural resource management, understanding the average processes is not always sufficient: decision-makers are increasingly more interested in having a realistic picture of all possible outcomes (Burgman, 2005; Power and McCarty, 2006) and associated uncertainties (O'Hagan, 2012).

It is therefore clear that some open questions still remain for a complete understanding of the uncertain impacts of climate change on water quality. These include how to quantitatively assess the conjoined effect of multiple stressors on the same endpoints; and how to develop integrative tools able to explicitly

deal with the uncertainty in climate change projections, accounting for the effect of anthropic changes and of different policy and adaptation measures (Sperotto et al., 2017; Terzi et al., 2019).

In order to fill these gaps, in this study we propose an integrated assessment procedure based on BNs to assess the potential implication of climatic changes (i.e. changes in precipitation and temperature, irregularities in water regime) and anthropogenic activities (i.e. land use, agronomic practices) on the quality of waters in the Zero river basin, one of the main tributaries of the Venice Lagoon (Italy).

Bayesian Networks (BNs) represent widely applied tools in environmental and water resources management (Aguilera et al., 2011; Landuyt et al., 2013; McCann et al., 2006; Newton, 2009; Phan et al., 2016), with great potentials of application also in the context of climate change impact assessment (Catenacci and Giupponi, 2010; Franco et al., 2016; Molina et al., 2013; Sperotto et al., 2017) thanks to their capability of capturing uncertainty and comparing the casual power of multiple stressors on the valued resource (Carriger et al., 2016; Landis et al., 2013).

Main aims of the work are to demonstrate the potentials of BNs (i) to understand future dynamics of nutrients loadings at river basin scale; (ii) to assess the interactive impacts of multiple stressors on water quality indicators); (iii) to develop alternative "what-if" risk scenarios to communicate the probability of changes in nutrients (i.e. $NO_3^-$, $NH_4^+$, $PO_4^{3-}$) delivered from the basin into the Venice lagoon, given a set of plausible future climate projections.

BNs were thus used as integrative tool for structuring and combining the information available from previous hydrological model simulations (i.e. SWAT) (Pesce et al., 2018), climate change projections, current land use and agronomic practices and historical observations, thus providing a valuable operative decision support tool directly usable by decision makers, water managers and non-experts to: i) understand and explore climate change impacts on water quality; ii) identify and prioritize most effective management and adaptation strategies to maintain good water quality status, in line with the

requirement of Water Framework Directive and other national legislation, under climate change conditions.

After a brief introduction to the case study area (Section1) the paper describes the methodological steps and input data used to implement the risk assessment procedure (Section 2) and finally, discusses the scenarios developed for the Zero river basin case study (Section 3).

## 1. Case study area

The Zero river basin (ZRB) (Figure 1, Table 1) , it is located within the Venetian floodplain (Northern Italy) and it is a sub-basin of the Venice Lagoon Watershed (Figure 1a). The Zero river (Figure 1b), which is 47 km long, originates near “San Marco di Resana”, and along its way, it collects the waters of numerous tributaries (e.g. Brenton del Maglio, Scolo Vernise, Rio Zermason). Then it merges with the Dese river about 2 kilometres upstream the discharge into the Venice Lagoon.

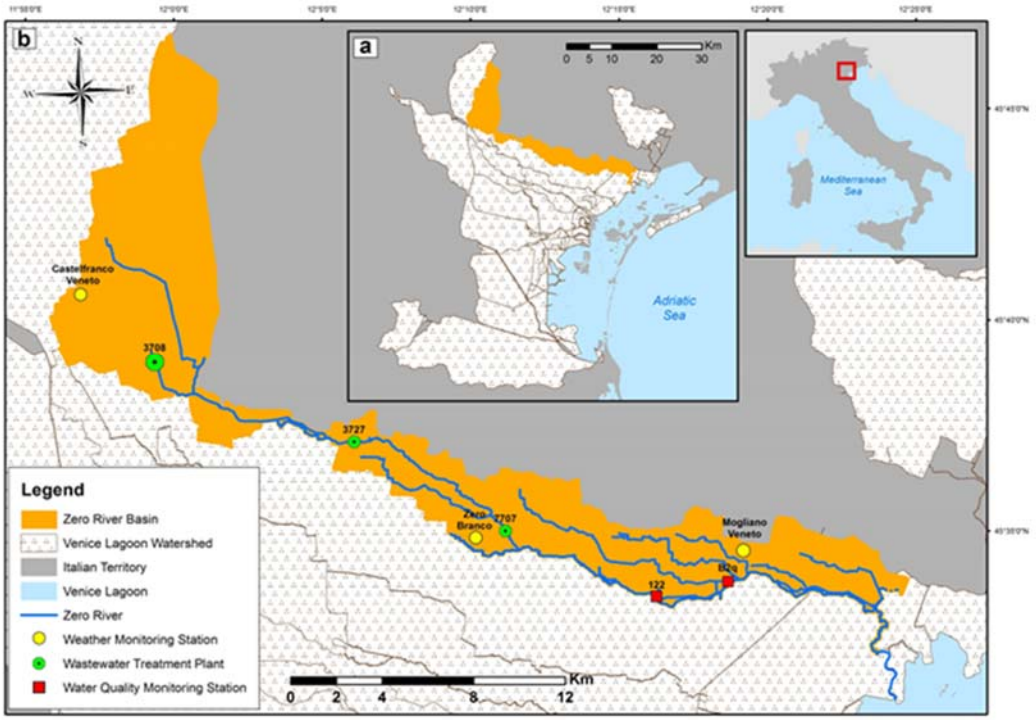


**Figure 1 The Zero river basin case study**

Overall, the Dese and Zero rivers together provide the greatest contribution of freshwater (21% of the total) to the lagoon of Venice (Zuliani et al., 2005). Thanks to its transitional position the basin features a Mediterranean climate but with typical traits of more Continental climates (Guerzoni and Tagliapietra, 2006) (Table 1). Thus, this climate is characterized by cold winters and generally well distributed precipitation throughout the year, with peaks in spring-autumn and minimums during the winter-summer periods Summers are frequently characterized by intense storms of short duration (Guerzoni and Tagliapietra 2006). The region features a marked inter-annual climate variability, which can originate years climatologically very different from each other.

**Table 1 Main climatic, environmental and socio-economic features of the Zero river basin**

| | |
|---|---|
| Location | Latitudes 45°28'N-45°48'N, longitudes 11°54'E-12°25'E; |
| Extension | 140 $km^2$; |
| Climate | Average annual precipitation=1000 mm (period 2007-2012);<br>Average annual temperature of 14 °C (period 2004-2013); |
| Land use | ▪ Agricultural areas (73%): corn (45%) (i.e. Zea mays L.), soy (9%) (i.e. Glycine max L.), autumn-winter cereals (13%) (i.e. Triticum aestivum L., Hordeum vulgare L.);<br>▪ Artificial areas (24%): housing areas (54%), industrial businesses (32%), transportation and services (14%);<br>▪ Semi-natural and forested areas (4 %) |

The environmental and the hydrological characteristics of the ZRB are heavily influenced by natural phenomena and human activities that together had shaped a complex hydrologic network. The basin, in fact, is characterised by several hydraulic infrastructures and artificial channels developed to reclaim land for agricultural purposes and to regulate the flow discharging into the lagoon of Venice (CVN, 2006). Furthermore, spring waters originated and risen in the surrounding areas influence the hydrology of the Zero river with the main contribution coming from an unconfined aquifer system located on the high plain (Servizio Acque Interne, 2008).

Main socio-economic activities insisting in the ZRB is are represented by agriculture, housing and industry (Table 1).

Moreover, three waste water treatment plans (i.e. Morgano, Zero-Branco and Castelfranco Veneto) (Figure 1b) with capacities ranging from 2500 to 32000 of Population Equivalents (P.E.) directly discharge into the Zero river.

The intensive agriculture, characterized by an elevated level of fertilization, and the dense urbanization are considered significant pollution sources for the area; especially for what concern nutrients (i.e. phosphorous, nitrogen) loadings. Diffuse and point nutrients pollution has become a major concern in the area since late 1980s when eutrophication reached its peak in the Venice Lagoon (Facca et al., 2014). Since then several national and regional policies, legislation and measures have been implemented to support investments for pollution control. Furthermore, good agricultural practice in concert with the Common Agricultural Policy (CAP) and other European regulations and directives has been implemented. In fact, the area has been identified as a Nitrate Vulnerable Zone (NVZ) according to the Nitrate European Directive (1991/676/CEE), with the aim of regulating and controlling the input of fertilizers from agricultural activities. At the same time, limits for the Maximum Admissible Load of nutrients discharged into the lagoon from the drainage basin were fixed at 3000 t/year for nitrogen and 300 t/years for phosphorous by the national competent law (DM 09/02/1999).

## 2. Material and methods

The risk assessment framework proposed in this work aims to assess the interactive effect of climate and anthropogenic changes on nutrients loadings. To do so, we adopt a multi-disciplinary approach to which different knowledge domains (i.e. environmental and social science, agronomy, hydrology, climate change) contribute. Also, quantitative and qualitative data, coming from multiple information sources, are integrated in a harmonic manner trough BNs. Accordingly, the proposed risk assessment approach is made upon different integrated components in communication through a dynamic exchange of information (Figure 2).

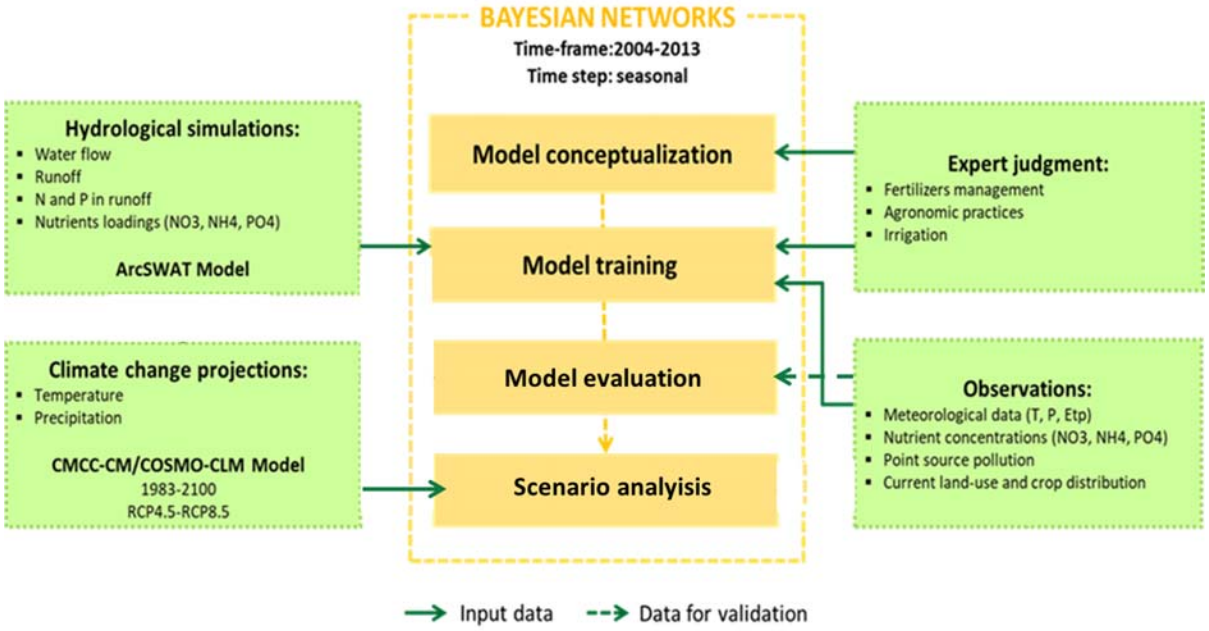


**Figure 2 General risk assessment framework applied to evaluate the interactive effect of climate and anthropogenic changes on nutrients loadings**

The core is the BN, which is used as meta-modelling tool for structuring and combining, into a probabilistic form, information provided by hydrological models, climate change projections, historical observations and expert judgment. Different information types populate the BN at different level of implementation. Qualitative information elicited from experts is used to develop the conceptual model of the network and to train socio-economic and agronomic variables of the model for which quantitative data are not available. Historical observations are used as input for the training of the network together with some hydrology and nutrient loadings variables provided by the hydrological simulation with the Soil and Water Assessment Tool *(*SWAT) (Arnold et al., 2012) for current conditions (Pesce et al., 2018). In addition, an independent set of observations is used for validation. After the training, climate change projections are employed as input for scenarios analysis to simulate the effect of future climate change on nutrients loadings.

Main outputs of the risk assessment approach are the values of key state and management variables for alternative risk scenarios, developing taking into account both projected climatic and not climatic conditions and that could be useful to support the identification of appropriate adaptation strategies at the local scale.

**2.1 Input data**

The capacity of the BN to correctly represent hydrological and water quality processes of the case study area strongly depends on the quality and completeness of input data. Accordingly, Table 2 summarizes the data collected for the implementation and evaluation of the risk assessment framework in the Zero river basin case study including three main typologies of data: observations, SWAT simulations and climate change projections.

Observations regarding the main climatic parameters (i.e. precipitation, temperature and evapotranspiration) and point-source pollution sources (i.e. wastewater treatment plants (WWTP) and industrial discharges) together with SWAT model simulations (i.e. runoff, river discharge (Q)) for the current conditions developed by (Pesce et al., 2018) for the case study were used for the training of the network for the period 2004-2013. More details about the calibration and validation processes applied to develop the SWAT model simulations used as input in this study can be found in Pesce et al., (2018).

Additional observed hydrologic data (i.e. river discharge (Q), nutrient concentrations (i.e. $NO_3^-$, $NH_4^+$, $PO_4^{3-}$) were only available for the period 2007-2012 and, therefore, were used to evaluate the performance of the model under current conditions.

Future daily precipitation and temperature projections were obtained by General Circulations Model/Regional Climate Model (GCM/RCM) nested simulations. Given the small extent of the study area and in order to represent correctly the spatial variability of climate conditions the CMCC-CM/COSMO-CLM

simulations were selected among those available with the highest spatial resolution. Specifically, precipitation and temperature simulations were obtained coupling the GCM CMCC-CM (Scoccimarro et al., 2011), with a spatial resolution of 0.75° x 0.75°, with the RCM COSMO-CLM (Rockel et al., 2008) under the configuration adapted to the Italian territory (Bucchignani et al., 2016; Cattaneo et al., 2012) with a spatial resolution of 0.0715° x 0.0715° (≈8km x 8km). CMCC-CM/COSMO-CLM simulations were evaluated using different independent set of observations (i.e. E-OBS, EURO4M-APGD and regional precipitation stations data) providing a good agreement with observed data and thus allowing a satisfactory representation of the Italian climate for both temperature and precipitation. A detailed description of COSMO-CLM evaluation results over the whole Italian domain can be found in Bucchignani et al. (2016) and Cattaneo et al. (2012) and in the Supplementary Material (SM) (Annex VI).

According with the purpose of the study, simulations developed using two different Representative Concentration Pathways (RCPs) (IPCC, 2013), respectively the RCP4.5 and RCP8.5 were considered. The RCP4.5, often referred as the "moderate" emission scenario which predicts an increase in radiative forcing up to 4.5 W m-2 by 2100 and a stabilization of the emissions (i.e. 650 ppm) shortly after 2100 (Thomson et al., 2011). RCP8.5, the "extreme" emission scenario, in which the GHGs emissions and concentrations increase considerably over the 21st century, leading to a radiative forcing of 8.5 W m-2 by 2100 (Riahi et al., 2011) thus describing a future without any specific climate mitigation target.

**Table 2 List of input data used for the application of the risk assessment model in the Zero river basin**

| Data type | Description | Time scale | Resolution | Source |
|---|---|---|---|---|
| **Observations** | | | | |
| Land cover map | ▪ Land use map of the Veneto region | 2006 | 1:10.000 | Regione del Veneto – Infrastruttura dati territoriali (http://idt.regione.veneto.it/app/metacatalog/) |
| Climatic Data | ▪ Daily precipitation<br>▪ Max/min daily temperature<br>▪ Daily evapotranspiration | 2004-2013 | 3 stations (i.e. Castelfranco, Veneto, Zero Branco, Mogliano Veneto) (Fig.1) | ARPAV – Servizio Meteorologico |

| | | | | |
|---|---|---|---|---|
| Water quantity and quality data | ▪ Observed daily river discharge<br>▪ Observed nutrients' ($NO_3^-$, $NH_4^+$, $PO_4^3$) concentrations in the lagoon | 2007-2012 | 2 stations (i.e. Manual station (Code 122), Automatic station (Code: B2q) (Fig.1) | ARPAV – Servizio Acque Interne<br>MAV – Magistrato Acque Venezia |
| Point-source pollution | ▪ Monthly N and P loadings from WWTP and Industrial discharges | 2004-2013 | 3 stations (i.e. Morgano, Zero-Branco, Castelfranco Veneto) (Fig.1) | ARPAV – Servizio Acque Interne |
| **Hydrological simulations** | | | | |
| Water quantity and quality data | ▪ Simulated runoff<br>▪ Simulated N and P load in the runoff | 2004-2013 | River basin | SWAT simulations (Pesce et al., 2018) |
| | ▪ Simulated river discharge Simulated nutrient loadings ($NO_3^-$, $NH_4^+$, $PO_4^{3-}$) in the lagoon | 2004-2013 | 1 station (i.e. Manual station (Code 122) | |
| **Climate change projections** | | | | |
| Climatic data | ▪ Temperature<br>▪ Precipitation | 1976–2100 | 8 km | CMCC-CM/COSMO-CLM simulations (Cattaneo et al., 2012; Scoccimarro et al., 2011) |

## 2.2 Bayesian Network development

BNs are probabilistic graphical models that represent a set of random variables and their interdependencies via conditional probability distributions (Nielsen and Jensen, 2009). BNs consist of three main elements: (i) a set of variables that represent the factors relevant to a particular environmental system (i.e. nodes); (ii) the relationships between these variables that quantify the links between variables (i.e. arcs); iii) Conditional Probability Tables (CPTs), indicating the strengths of the links in the graph by denoting the likelihood of the state of a 'child' node given the states of its 'parent' nodes (Landuyt et al., 2013). The DAG consists of a set of nodes that can take on a number of pre-defined discrete "states", which are mutually exclusive and exhaustive (Borsuk et al., 2004).

Bayesian Networks rely on Bayes' theorem of probability theory to propagate information between nodes allowing to update or revise the beliefs of the probabilities of system states taking certain values, in light of new evidences. Accordingly, in Bayes' theorem, a prior probability represents the likelihood that an input variables will be in a particular state; the conditional probability calculates the likelihood of the state of a variable given the states of input variables affecting it; and the posterior probability is the likelihood that variable will be in a particular state, given the input parameters, the conditional probabilities, and

the rules governing how the probabilities combine. The network is solved when all nodes posteriori probabilities have been calculated using Bayes' Rule:

$$P(A|B) = \frac{P(B|A)\,P(A)}{P(B)} \quad \text{(Equation 1)}$$

where P(A) is the prior distribution of parameter A; P(A|B) is the posterior distribution, the probability of A given new data B; P(B|A) the likelihood function, the probability of B given existing data A. The BN for the Zero river basin was implemented and run using the software HUGIN Expert, version 8 (Bromley et al., 2005; Madsen et al., 2005). The development of a BN is an iterative and adaptive process which consist in four major steps: i) the development of the conceptual model of the system; ii) the training of the model with data; iii) the evaluation of model performances; and finally, iv) scenario analysis (Kragt, 2009) (Figure 2). Accordingly, the following Sections describe how the different BNs development phases have been implemented in the Zero river basin case study.

### 2.2.1 Development of the conceptual model of the system

The phase of model conceptualization aims at developing an influence (i.e. "box and arrow") diagram providing a graphical representation of the system under consideration. The network conceptualization, therefore, includes the identification of the main system variables (i.e. nodes) as well as the links between them (i.e. directed arcs). The identification of relevant variables and links can be typically based on a literature review, expert knowledge and consultation with local stakeholders. For each variable, appropriate indicators as much as possible measurable, observable and predictable have to be identified. Once the variables and relative indicators are defined, the links between them are identified and represented as unidirectional arrows as BNs do not permit feedback loops. Figure 3 provides a representation of the influence diagram developed for the Zero river case study which was developed

based on expert consultation following the DPSIR (Driving forces, Pressures, States, Impacts and Responses) framework (EEA, 1999; Kristensen, 2004). The DPSIR here was adopted to conceptualize the system identifying the main cause-effect relationships and interactions between climatic changes, actual land use and the quality of water resources.

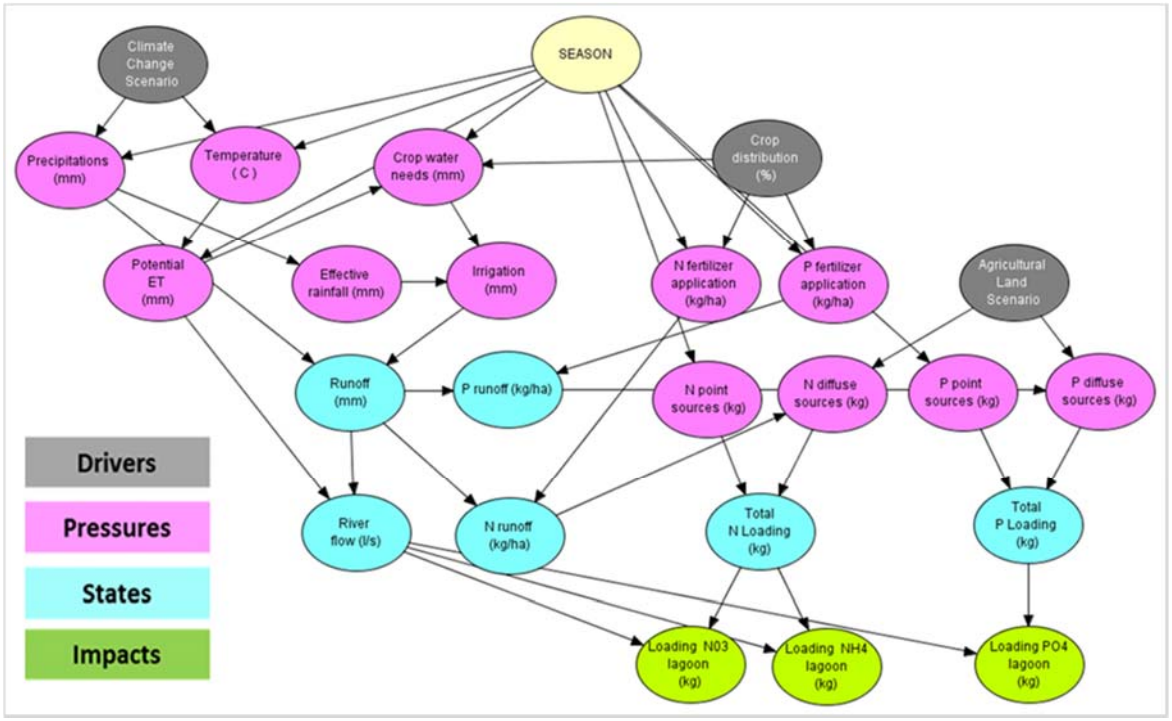


**Figure 3 Conceptual model of the system developed for the Zero river basin**

Accordingly, different kind of nodes representing the different nature of variables involved have been included in the BN (Figure 3):

- **Driver nodes (grey)**, consist in the input or parent nodes of the network and include environmental and socio-economic factors representing the main drivers of water quality alterations. Accordingly, in this study, driver nodes include climate change scenarios, agricultural

land scenario (i.e. alternative agricultural land extension) and crop distributions (i.e. alternative combination of different percentage of crop typologies).

- **Pressures nodes (violet)**, represent the variables which are influenced by the identified drivers. Precipitation, temperature and potential evapotranspiration's will depend on the climate change scenario, inducing certain pressures on the system, including alternations in water needs for the different crops which, together with a reduced effective rainfall, will mostly lead to an increased water demand for irrigation. On the other hand, regarding anthropogenic drivers, crop typology distributions will drive irrigation demand but also the quantity and timing of fertilizer application (i.e. N and P fertilizer application), affecting the loading of nitrogen and phosphorous entering in the system through diffuse (i.e. N and P diffuse sources) and non-diffuse sources (i.e. N and P point sources).

- **States nodes (blue)**, representing the characteristics (i.e. states) of water resources that can be altered by the aforementioned pressures both in quantitative and qualitative terms. Quantitative alterations include, in this study, the alteration of river flow and runoff as results of changes in precipitation and temperature under different climate change scenarios. Qualitative alterations are instead represented by the change of N and P loadings in the runoff and in the increase of the total loading of N and P into the river resulting from the interaction between multiple climatic and anthropogenic pressures.

- **Impact nodes (green),** consist in the output or child nodes of the network and are represented by the increase of nutrients loadings (i.e. $NO_3^-$, $NH_4^+$, $PO_4^{3-}$) discharged by the Zero river basin into the Venice Lagoon which can have severe impacts on the environment and human activities.

### 2.2.2 Model training

The second step regards models training and involves assigning states, prior and conditional probabilities to all nodes of the networks, thus translating the conceptual model developed in Section 2.2.1 (Figure 3) into probabilistic results. For each node a certain number of states must be identified. States represent potential values or conditions that the variable can assume in the analysed system (Kragt, 2009) and can be featured in different way, representing Boolean functions (e.g. true, false), categorical definitions (e.g. low, medium, high), continuous or discrete numeric intervals (de Santa Olalla et al., 2005).

Once the type and number of states have been defined, the prior probability associated to each state of the node have to be calculated based on available information and knowledge (Pollino et al., 2007). Prior probability is the likelihood that a node will be in a particular state before some evidence is taken into account and thus represent the best rational assessment of the probability of an outcome based on the current knowledge (Pollino and Henderson, 2010). Accordingly, the prior probability distribution describes the starting point for each node in the network and thus the expectation of the node being in a certain condition given current knowledge and data.

Finally, to operationalize the network, Conditional Probabilities (CPs) of nodes have to be specified for all combinations of states of its parent nodes. Specifically, CPs of an event B is the probability that the event will occur given the knowledge that an event A has already occurred and is calculated using Equation 2:

$$\mathrm{P(B|A)} = \frac{P(A \text{ and } B)}{P(A)} \quad \text{..... (Equation 2)}$$

Where P(B|A) is the conditional probability of B given A, P (A and B) is the probability that both events A and B occur, P(A) is the probability of A is occurring.

CPs calculated using Equation 2 are represented in the Conditional Probabilities Table (CPTs) of every node which display conditional probabilities of a single variable with respect to the others (i.e., the probability

of each possible value of one variable if we know the values taken on by the other variables) and thusthe strength of relationships between the systems' variables.

If a node has no parents (i.e. input nodes), it can be described probabilistically by a marginal probability distribution. CPTs for each node can be defined using a range and combination of methods including observed data, probabilistic or empirical equation, results from model simulation or elicitation from expert knowledge (Pollino and Henderson, 2010). Within this study, states, prior probability distribution of nodes as well as the conditional probability distributions have been defined combining different quantitative and qualitative information available for a training period of 10 years (i.e. 2004-2013) at a seasonal time-step. Table 3 describes the states of the different nodes of the network and the type of information and data, which have been used for the definition of prior and conditional probability distributions. Most nodes present numerical interval type states, which have been identified starting from existing observed dataset, model simulation or expert judgement. Specifically, for each numeric interval nodes, continuous numerical dataset (i.e. series of observation or model simulations) have been discretized into states dividing the range between the maximum and the minimum values of the series into four intervals of equal amplitude (Table 3). For the labelled node types, instead, states have been defined based on the alternative conditions the node can assume (i.e. alternative seasons, alternative climate change scenarios) (Table 3).

**Table 3 Overview of nodes and states in the Bayesian Network model for the Zero river basin**

| Node | Description | Type | States | Parametrization method |
|---|---|---|---|---|
| Season | Alternative seasons | Labelled | Winter | Expert judgement |
| | | | Spring | |
| | | | Summer | |
| | | | Autumn | |
| Climate change scenario | Alternative climate change scenarios | Labelled | Baseline 1983-2012 | CMCC-CM/COSMO-CLM simulations |
| | | | RCP 4.5 2041-2070 | |
| | | | RCP 4.5 2071-2100 | |
| | | | RCP 8.5 2041-2070 | |
| | | | RCP 8.5 2071-2100 | |
| | | Labelled | Actual 2004-2013; | |

| Node | Description | Type | States | Parametrization method |
|---|---|---|---|---|
| Agricultural land scenario | Extension of land (ha) occupied by agricultural activities under different scenarios | | Future 2050 | Observations-LUISA simulations |
| Temperature | Seasonal average temperature (°C) | Numeric interval | 0-8.37 | Observations |
| | | | 8.37-13.79 | |
| | | | 13.79-19.21 | |
| | | | >19.21 | |
| Precipitation | Seasonal cumulative precipitation (mm) | Numeric interval | 0-201.50; | Observations |
| | | | 201.50-328.73 | |
| | | | 328.73-455.96 | |
| | | | > 455.96 | |
| Potential ET | Seasonal cumulative potential evapotranspiration (mm) | Numeric interval | 0-133.85 | Observations |
| | | | 133.85-228.3 | |
| | | | 228.3-322.75 | |
| | | | >322.75 | |
| Effective rainfall | Seasonal cumulative effective rainfall reaching the soil (mm) | Numeric interval | 0-64.13 | SWAT simulations |
| | | | 64.13-122.95 | |
| | | | 122.95-181.77 | |
| | | | >181.77 | |
| Crop water needs | Seasonal water demand for different crop typology (mm) | Numeric interval | 0-109.77 | Equation (Annex I, SM) |
| | | | 109.77-213.64 | |
| | | | 213.64-317.50 | |
| | | | >317.50 | |
| Irrigation | Seasonal amount of water applied as irrigation | Numeric interval | <-55.29 | Equation (Annex I, SM) |
| | | | -55.29-101.28 | |
| | | | 101.28-257.86 | |
| | | | >257.86 | |
| N fertilizer application | Nitrogen fertilizer applied for each season according to different crop typology (kg/ha) | Numeric interval | 0-45.74 | Expert judgment |
| | | | 45.74-87.52 | |
| | | | 87.52-129.30 | |
| | | | >129.30 | |
| P fertilizer application | Phosphorous fertilizer applied for each season according to different crop typology (kg/ha) | Numeric interval | 0-25.41 | Expert judgment |
| | | | 25.41-50.83 | |
| | | | 50.83-76.25 | |
| | | | >76.25 | |
| N diffuse sources | Seasonal amount of nitrogen coming from agricultural practices (kg) | Numeric interval | 0-7388.86 | Equation (Annex I, SM) |
| | | | 7388.86-13959.99 | |
| | | | 13959.99-20531.11 | |
| | | | >20531.11 | |
| P diffuse sources | Seasonal amount of phosphorous coming from agricultural practices (kg) | Numeric interval | 0-5169.28 | Equation (Annex I, SM) |
| | | | 5169.28-10221.75 | |
| | | | 10221.75-15274.21 | |
| | | | >15274.21 | |
| N point sources | Seasonal amount of nitrogen coming from point sources (i.e. Waste Water Treatment Plans and Industrial discharges) (kg) | Numeric interval | 0-9382.64 | Observations |
| | | | 9382.64-10389.82 | |
| | | | 10389.82-11396.99 | |
| | | | >11396.99 | |
| P Point sources | Seasonal amount of phosphorous coming from point sources (i.e. WWTPs and Industrial discharges) (kg) | Numeric interval | 0-1143.64 | Observations |
| | | | 1143.64-1478.99 | |
| | | | 1478.99-1814.35 | |
| | | | >1814.35 | |
| River discharge | Seasonal average river discharge (l/s) | Numeric interval | 0-1458.96 | SWAT simulations |
| | | | 1458.96-2360.53 | |
| | | | 2360.535-3262.102 | |
| | | | > 3262.10 | |
| Runoff | Seasonal cumulative runoff (mm) | Numeric interval | 0-49.90 | SWAT simulations |
| | | | 49.90-90.15 | |
| | | | 90.15-130.40 | |
| | | | >130.40 | |
| N in runoff | | Numeric interval | 0-0.63 | SWAT simulations |

| Node | Description | Type | States | Parametrization method |
|---|---|---|---|---|
| | Seasonal amount of nitrogen loaded in the runoff (kg/ha) | | 0.63-1.19 | |
| | | | 1.19-1.75 | |
| | | | >1.75 | |
| P in runoff | Seasonal amount of phosphorous loaded in the runoff (kg/ha) | Numeric interval | 0-0.44 | SWAT simulations |
| | | | 0.44-0.87 | |
| | | | 0.87-1.30 | |
| | | | >1.30 | |
| Total N loading | Seasonal nitrogen load in the river (kg) | Numeric interval | 0-17031.20 | Equation (Annex I, SM) |
| | | | 17031.20-24401.92 | |
| | | | 24401.92-31772.64 | |
| | | | > 31772.64 | |
| Total P loading | Seasonal phosphorous load in the river (kg) | Numeric interval | 0-5405.76 | Equation (Annex I, SM) |
| | | | 5405.76-9710.91 | |
| | | | 9710.91-14016.07 | |
| | | | >14016.07 | |
| Loading $NO_3^-$ lagoon | Seasonal loading of $NO_3$ reaching the lagoon (kg) | Numeric interval | 0-28047.50 | SWAT simulations |
| | | | 28047.50-48615.00 | |
| | | | 48615.00-69182.50 | |
| | | | >69182.50 | |
| Loading $NH_4^+$ lagoon | Seasonal loading of $NH_4^+$ reaching the lagoon (kg) | Numeric interval | 0-3224.52 | SWAT simulations |
| | | | 3224.52-5009.3 | |
| | | | 5009.3-6794.17 | |
| | | | >6794.17 | |
| Loading $PO_4^{3-}$ lagoon (kg) | Seasonal loading of $PO_4^{3-}$ reaching the lagoon (kg) | Numeric interval | 0-1978.90 | SWAT simulations |
| | | | 1978.90-2954.00 | |
| | | | 2954.00-3929.10 | |
| | | | >3929.10 | |

As described in Table 3 for most nodes prior probability and conditional probability distributions have been extrapolated directly from the observed frequencies of the corresponding variable. For nodes associated with climatic variables (i.e. temperature, precipitation, evapotranspiration), probabilities have been learned from the frequencies of observations of weather monitoring stations available in the case study (Section 2.1. Probabilities distribution of hydrological variables (i.e. runoff, river flow, nutrients loadings, N and P in the runoff), instead, have been calculated based on the frequency analysis of the results of hydrological simulations performed with the SWAT model (Section 2.1). Finally, for nodes describing agronomic practices (i.e. water needs, irrigation, P and N fertilizer application), due to the lack of quantitative information in the case study, the CPs were calculated through expert elicitation and applying empirical equations. An exhaustive description of assumption and information used to parametrize CPs of such nodes can be found in Annex I (SM). Figure II1 Annex II (SM) show the

configuration of the BN for the Zero river basin once states, prior and conditional probabilities of each node have been parametrized.

### 2.2.3 Model evaluation

A fundamental aspect in BNs developed to support risk assessment and decision making is model evaluation. This steps is crucial as it allows to quantify the performance of the model and to assess the achievement of the purposes for which it was designed (Kragt, 2009). According to Pollino and Henderson (2010), two main form of model evaluation should be performed on BNs including the model predictive accuracy assessment and sensitivity analysis.

#### 2.2.3.1 Predictive accuracy and uncertainty analysis

Predictive accuracy refers to the quantitative evaluation of the BN results, comparing model predictions with observed data. Within this study, the ability of the BN to correctly predict instances on independent data was investigated comparingBN simulations with observations from water quality monitoring stations available for the case study (Section 3.2). Accordingly, for each output node (i.e. NO3, NH4 and PO4 loadings) Correctly Classified Instances (CCI) were assessed as the percentage of cases correctly predicted divided by the total number of cases, providing the measures of how many instances the model predicts correctly when tested against know cases outcomes (i.e. observations). Error rates, used as evaluation criteria, were then computed and depicted in the so-call confusion matrices as suggested in (Marcot, 2012).

In addition, the Receive Operating Characteristics (ROC) curves (Hand, 1997) were calculated using HUGIN. ROC curves plot the percent true positive as a function of their complement, percent false positive, and accordingly the area under the ROC curve (AUC), ranging from 0 to 1, can be used as metric

to judge the performance of predictive models where 1 denotes no error while 0.5 denotes totally random models (Marcot, 2012).

Since the probability distribution of each node is a depiction of uncertainty itself, the uncertainty in BN outputs was captured analyzing the Variance ($\sigma^2$) and the Entropy (H(X)) of the probability distribution of output nodes. While the Variance represent the dispersion or spread of the outcomes around the mean, and can be quantitively expressed using the Standard Deviation (SD), the Entropy can be seen as a score of a variable richness (i.e. how much information is within the data for that particular variable) (Pearl, 1988; Pollino et al., 2007).Entropy expresses the measures of the associated uncertainty of the random process that a particular probability distribution describes (Molina et al., 2016) and is calculated using the function:

$$H(x)=-\sum P(x) \log P(x) \quad \text{(Equation 3)}$$

Reducing entropy by collecting information, in addition to the current knowledge about the variable x is interpreted as reducing the uncertainty about the true state of x. Accordingly, the entropy function enables an assessment of the level of uncertainty/certainty about the state of output node and of the additional information required to specify a particular alternative.

**2.2.3.2 Sensitivity analysis**

Another form of evaluating the developed model consist in the sensitivity analysis which allow to test the sensitivity of model outcomes to variations of model parameters (Kragt, 2009). In the context of BN sensitivity analysis help in exploring the behaviour of the system and assessing the model sensitivity to different input variables. Through sensitivity analysis, in fact, it is possible to detect how the variation in the output of a model can be apportioned to different variations in the inputs and thus track relevant

causal pathways between variables. Accordingly, sensitivity to parameters was analysed to identify the most influential set of variables (i.e. those have the greatest influence on the model endpoints), as well as to rank the relevance and strength of inputs nodes on model output (i.e. nutrients loadings).

The analysis was performed adopting an empirical approach in which the input parameters were modified one by one and the related changes in the output parameters were observed (Coupé et al., 1999; Pollino et al., 2007; Stelzenmüller et al., 2010). Results of data-based evaluation and sensitivity analysis for the developed BN are described and discussed in Sections 3.1.

### 2.2.4 Scenario analysis

Once the BN was trained, the resulting model can be used to analyse the performance of the system under different scenarios. This allows to assess the relative changes in the posteriori probabilities of output nodes (e.g. nutrient loadings) when altering the probability distribution of one or more input nodes (e.g. climate change scenarios). A common manner to develop scenarios using BNs is to "set evidence" for one or more nodes (e.g. assigning 100% probability for one state) and thereby, let the information propagating through the nodes that are linked by CPTs in the network (Kragt, 2009).

In this study, we were interested in assessing the effect of future climate change scenarios on nutrient loadings and therefore, five 30-year scenarios were developed, including a control period (1983-2012), a mid-term (2041-2070) and long-term (2071-2100) scenarios under two different representative concentration pathways (i.e. RCP4.5-RCP8.5).

Accordingly, for each climate change scenario the probability distribution of temperature and precipitation was calculated based on the respective CMCC-CM/COSMO-CLM model simulations (Section 2.1.2) and set as evidence in the input nodes. Figure II2 Annex II (SM) provide an example of scenario

analysis using the BN while a quantitative discussion of the results of BN simulations with other climate change scenarios is provided in Section 3.1.

# 3. Results

## 3.1 Model evaluation

### 3.1.1 Data-based evaluation and uncertainty analysis

As described in Section 2.2.3.1 a data-based evaluation was performed to assess the ability of the model to correctly predict instances on independent dataset. Accordingly, BN predictions were tested against observations from water quality monitoring stations available from ARPAV for the case study (Table 1, Section 2.1) generating confusion matrixes representing the percentage of CCIs and consequently the error rates. Unfortunately, observations were available only for 2007-2012 and therefore the evaluation was conducted only for this period.

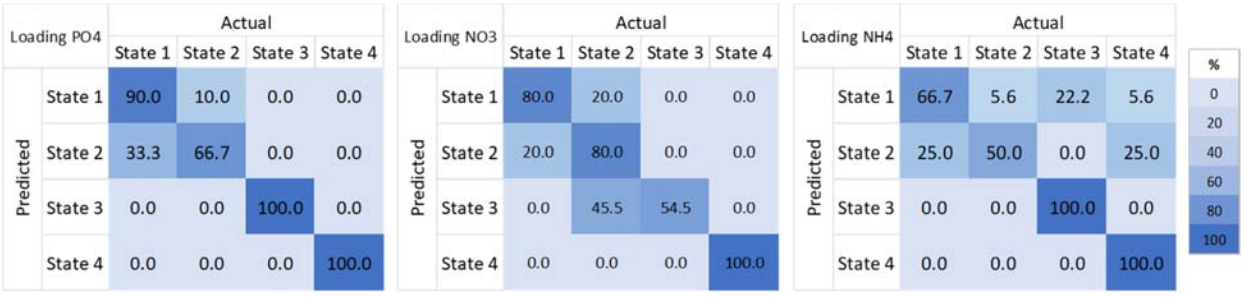


**Figure 4 Confusion matrixes for outputs nodes of BN model tested against observed dataset (2007-2012). The cells lying on the leading diagonal of the matrices represent correctly predicted instances while off diagonal are incorrect predictions. Colors bar represent classification rates in percentage.**

In addition, in order to make the outcome of the evaluation comparable, the probabilistic results have been translated into deterministic form (i.e. numerical value) and expressed using the Expected Value of the Probability distribution (Annex III, SM).

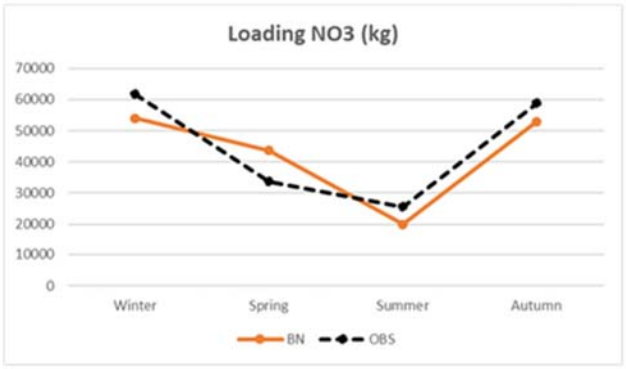


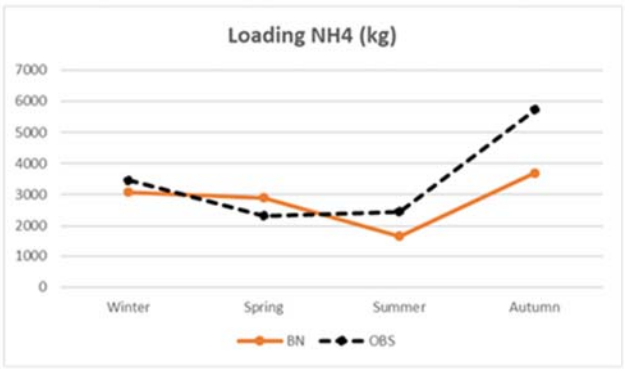


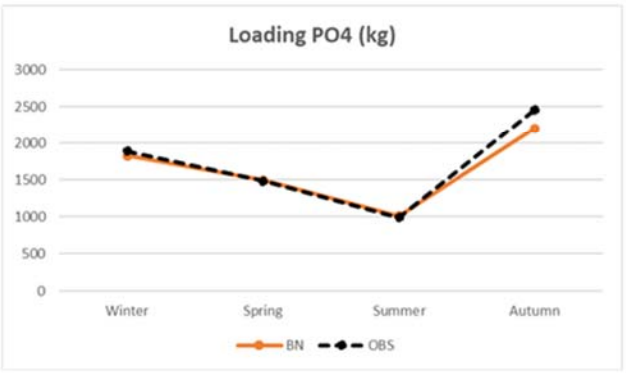


| | | | Winter | Spring | Summer | Autumn |
|---|---|---|---|---|---|---|
| NO3 | BN | μ | 53050.5 | 41944.5 | 24267.8 | 53530.7 |
| | | SD | 14594.5 | 18761.7 | 15491.9 | 13266.5 |
| | Obs | μ | 61703.3 | 33656.7 | 25554.2 | 58898.8 |
| | | SD | 26082.2 | 15671.7 | 17353.8 | 20567.5 |
| NH4 | BN | μ | 3189.1 | 2821.5 | 1818.8 | 3697.8 |
| | | SD | 1951.9 | 1603.1 | 832.1 | 2154.1 |
| | Obs | μ | 3459.5 | 2327.2 | 2447.2 | 5721.8 |
| | | SD | 1940.7 | 1598.6 | 1180.7 | 2482.0 |
| PO4 | BN | μ | 1834.1 | 1446.9 | 1012.4 | 2204.7 |
| | | SD | 957.8 | 879.8 | 211.3 | 1300.0 |
| | Obs | μ | 1890.5 | 1481.8 | 1012.4 | 2461.6 |
| | | SD | 957.8 | 696.3 | 211.3 | 1096.6 |

**Figure 5 Expected Value of the probability distributions of nutrient loadings ($NO_3^-$, $NH_4^+$, $P0_4^{3-}$) of observed data (black) and of Bayesian Network outputs (red) for the period 2007-2012.**

Overall, the BN was able to reproduce the observed nutrients dynamics with loadings closely replicated for most seasons. The evaluation produced very good results phosphorous ($PO_4^{3-}$) while for ammonium ($NH_4^+$) and nitrate ($NO_3^-$) the correlation between observed and predicted nutrient loadings was slightly worse. Indeed, overall the BN was able to classify correctly the 87.50% of instances for $PO_4^{3-}$, the 63.64% for $NH_4^+$ and the 66.67% for $NO_3^-$, when tested against the observed dataset (Figure 4).

BN overpredicts the decrease of ammonium and nitrate loadings between spring and summer while underestimates the autumn loadings (Figure 5) for all the three nutrients species (i.e. $PO_4^{3-}$, $NH_4^+$, NO3) and the winter loadings of $NH_4^+$ and $NO_3^-$. Good performance of BN model was also confirmed when

investigating ROC curves: also in this case $PO_4^{3-}$ present the better performance (ROC=0.88) followed by $NO_3^-$ (ROC=0.81) and $NH_4^+$ (ROC=0.73).

In general, observed and simulated probability distributions are similar and characterized by comparable Variance and Standard Deviations (Figure 5). Autumn and winter distributions present a higher spread around their expected value denoting a higher uncertainty in the outcome respect to summer.

Entropy results showed that "$NO_3^-$ Loading" is the output node presenting the less informative probability distribution (Figure V1, Annex V (SM)) being characterized by the highest total entropy values (i.e. 1.24) and thus by the highest level of uncertainty. Higher value of entropy resulted for autumn season for $NH_4^+$and $PO_4^{3-}$ loadings and for spring for $NO_3^-$ loadings while very low values of entropy are associated with summer probabilities distributions for all nutrients.

Uncertainty analysis confirmed the linear correlation between variance and entropy: probabilities distributions described by larger variance and SD are those of outputs nodes characterized by higher entropy and larger uncertainty.

**3.1.2 Sensitivity Analysis-Identification of most influencing variables**

Sensitivity analysis considering the sensitivity to parameters was performed to identify and prioritize variables that have the greatest influence on model outputs (i.e. nutrients loadings). Based on the empirical approach proposed by Pollino et al. (2007), each node was alternatively maximized by setting the probability of its higher state equal to 100% and, consequently the relative change in each of the other nodes was analysed. Magnitude of change was measured calculating the Percent Change of the Expected Value of the probability distribution of output nodes (i.e. $NO_3^-$, $NH_4^+$, $PO_4^{3-}$ loadings) according with the Equation IV.I (Annex IV (SM)) (Molina et al., 2016). Results (Table IV1, Annex IV (SM)) have been normalized into a 0-1 interval based on the minimum and maximum values obtained to make outcomes

immediately understandable and comparable. Results, summarized in the Figure 6, allowed to develop a ranking of input variables according with their relevance in the BN and consequently in the system. A higher Percent Change value denotes that the analysed variable has a high influence on the output variables (i.e. nutrient loadings), by contrary a lower value suggests a negligible effect.

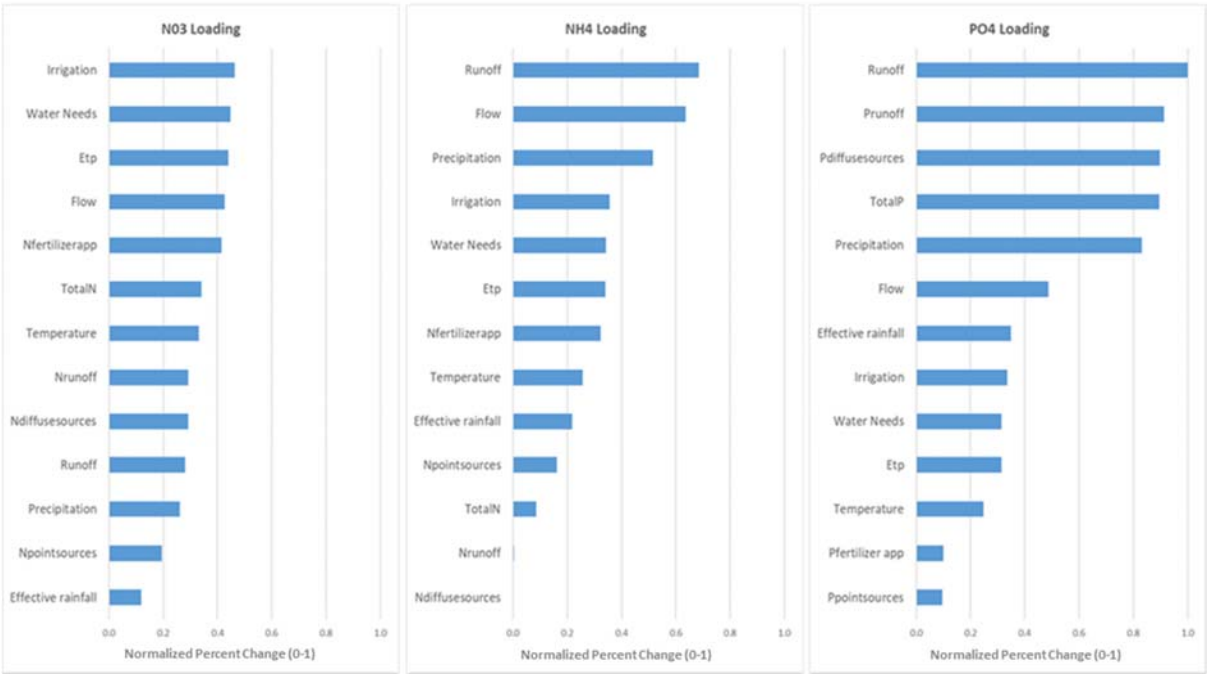


**Figure 6 Graphical representation of the results of the sensitivity analysis, represented as the normalized (0-1) percentage change of output variables (i.e. $NO_3^-$, $NH_4^+$, $PO_4^{3-}$ loadings).**

According to sensitivity analysis outcomes, $NO_3^-$ loadings are mainly driven by agronomic practices including irrigation, fertilizers application and water needs of crops which, in turn, is strictly related to crop potential evapotranspiration. All these variables, in fact, induced the higher percent change in the $NO_3^-$ loading node ranging from the 0.46 (51% change, Table IV1, Annex IV (SM)) for irrigation to the 0.41 (46% change, Table IV1, Annex IV(SM)) for N fertilizer application. Also, the river flow moderately influences the loading with 0.46 of percent change correspondent to 47% (TableIV1, Annex IV (SM)). Despite not being directly linked through the network, irrigation is the variable that mostly influence the

$NO_3^-$ loading. $NO_3^-$ is highly soluble in water and therefore is likely to be rapidly washed out by the water applied trough irrigation and to be transported in dissolved form through the river when the river flow is regular. The application of nitrogen fertilizers is usually higher during spring and summer, when higher are also water needs for summer crops (i.e. maize). Consequently, it could explain the concomitant influence of these agronomic variables in increasing $NO_3^-$ loadings.

The runoff is the variable that more strongly influence the $NH_4^+$ loading, inducing a 0.68 % change with a change of 76% of the Expected Value in the output node. Ammonium ($NH_4^+$) is not very soluble, however, the portion adsorbed to soil colloids can be transported into surface water during water erosion process induced by extreme runoff. River flow, being directly linked with the $NH_4^+$ loading in the network, have a moderate influence (i.e. 0.64 correspondent to 71% change (Table IV1, Annex IV (SM))

$PO_4^{3-}$ loading, instead, is strongly affected by the runoff, the loading of phosphorous into the runoff and consequently, by the intensity of diffuse pollution sources. In particular, the runoff causes the maximum variation (i.e. 1) corresponding with a percent change of 111% while the phosphorous in the runoff and phosphorous diffuse sources contribute respectively for the 102% and 101% percent of change (Table IV1, Annex IV, (SM)). High runoff intensity, mainly related to intense precipitation is recognized as one of the main factor influencing the transport of phosphorous from agricultural areas to water bodies (Lundekvam et al., 2003).

### 3.2 Quantitative assessment of seasonal nutrient loadings under climate change scenarios

Once trained and evaluated, the BN was used to perform scenario analysis to assess the effect of future climate change on nutrients loadings and hydrological variables. This was done by forcing the model with the 30-year seasonal distribution of temperature and precipitation for mid-term (2041-2070) and long-

term (2071-2100) projections under two different representative concentration pathways (i.e. RCP4.5-RCP8.5) according with the projections provided by the CMCC-CM/COSMO-CLM (Section 2.1).

Future projections of the CMCC-CM/COSMO-CLM show a general increase of temperatures in every season with the probability of medium (i.e. 8.36-13.76 °C), high (13.76-19.21 °C) and very high (>19.21 °C) temperature states that increase in all seasons and scenarios respect to the baseline 1983-2012 (Figure 7a). Maximum increases are reached by the RC8.5 2071-2100 scenario with a 76% probability of very high temperature state in spring and 50% probability of medium temperature state in autumn.

Differently, for precipitations, projections show a general decrease in spring and summer (Figure 7a). The probability of lower precipitation states (0-201 mm), in fact, increases across scenarios reaching the 90 % in the RCP8.5 2071-2100 in summer with an increase of 50% respect to the baseline 1983 (i.e. 43%). Despite the decrease, for scenario RCP8.5 2041-2070 in spring the probability of very high (i.e. >455 mm) and high (i.e. 328-455) precipitation states is remarkable (i.e. 8% and 10% respectively), denoting an increase in the probability of occurrence of extreme precipitation events during this season. In winter, future scenarios project a decrease in precipitation in the mid-term period follow by an increase over long-term and by the end of the century for both RCPs. The highest increase however will be registered in autumn with the probability of higher precipitation states (i.e. 328-455, >455 mm) that increase in all the scenarios and up to 30% in the long-term period for both RCPs.


**Figure 7 Probability distribution of temperature (a) and precipitation (b) for different seasons across climate change scenarios**

Changes in precipitation and temperature associated with different climate change scenarios induce changes in the main hydrological variables of the systems (e.g. river flow, runoff, N and P in the runoff). Figure 8 show the changes in the probability distribution of river discharge and runoff respect to the baseline (1983-2012) considering multiple climate change projections. In order to make the outcome of each simulated scenarios more understandable, the probabilistic results (Figure 8, left) have been also translated into deterministic form (i.e. numerical value) (Figure 8, right) and expressed using the Expected Value of the Probability distribution (Annex III, (SM)).


**Figure 8 Probabilistic (left) and deterministic (right) results for river discharge (a) and runoff (b) for different seasons across climate change scenarios**

BN predictions show an increase in both the runoff and river discharge in autumn and a clear decrease in spring and summer across different scenarios (Figure 8a, left).

In winter, instead, for both variables, the BN predicts a general decrease in the mid-term period follow by an increase over long-term and by the end of the century (Figure 8), strongly reflecting the changes in precipitation distribution (Figure 7a). Despite revealing a similar behaviour over future scenarios, the runoff presents the higher variation across all seasons respect to the baseline (Figure 8b, right) accordingly with its stronger dependency on precipitations (Figure 7a).

Specifically, in spring the probability of the lowest states (i.e. 0-49.90 mm) increase from the 10% of the baseline to the almost 50% in the in the baseline RCP8.5 long-term period (i.e. 2071-2100) while in summer from 64% to 92%. In autumn, greater increase in the runoff is predicted for the RCP8.5 2041-2070 scenario (Figure 8b, left) with a probability of 50% of being in the higher runoff states against the 20% of the baseline. For river discharge, instead, maximum increase is projected for the RCP8.5 2041-2070 in autumn (Figure 8a) with the probability of the highest river discharge state (i.e. >3263 l/s)) that increase from the 27% of the baseline (i.e. 1983-2012) to the 50% according with the maximum increase of precipitation in the same scenario (Figure 7a).

The climate, runoff and river discharge control the capability of the river basin to export nutrients and therefore their changes affect the amount of nutrients seasonally loaded in the lagoon.

The BN predicts changes in the seasonal distribution of $NO_3^-$ loadings respect to the current condition (i.e. 1983-2012) (Figure 9). Specifically, for future scenario it can be notice a shift in high $NO_3^-$ loadings with greater loadings occurring in autumn rather than in winter (Figure 9a). Both RCP4.5 and RCP 8.5 scenarios show a clear increase in autumn loads and a small decrease in both spring and summer loads. In autumn, in fact, the probability of high (i.e. 90.15-130.40 kg/season) and very high (i.e. >130.40 kg/season) loadings states increase across scenarios reaching respectively the 62% and 11% in the RCP4.5 2071-2100 scenario and the 67% and 10% in the RCP8.5 2041-2100 scenario (Figure 9a). Accordingly, in autumn, the greatest increase in $NO_3^-$ loadings is predicted under the long-term scenarios RCP4.5 2071-2100 and the medium-term scenarios RCP8.5 2041-2070 (Figure 9a) in correspondence with the greater increase in river flow

(Figure8a). In spring and summer greater reduction in $NO_3^-$ loading are predicted for scenario RCP8.5 2071-2100, the one also characterized by the greatest decrease in river flow (Figure 8a).

Regarding ammonium (i.e. $NH_4^+$), the projections show a slight decrease of loadings in spring and summer and an increase in autumn (Figure8b). Specifically, in autumn the probability of low loading state decreases gradually across scenarios followed by an increase in the probability of very high loadings (i.e. >6794 kg/season), which reaches a 22% under the RCP8.5 2041-2070 (Figure 9b). High loadings occur in correspondence with the highest projected runoff (Figure 8b), suggesting that this variable could play a major role in controlling the transport of $NH_4^+$.

Finally, seasonal changes in the phosphorous (i.e. $PO_4^{3-}$) loading have been also observed (Figure 9c). Results indicate a marked increase in autumn loads and a general decrease in spring and summer loads across scenarios. An exception is for the scenario RCP8.5 2041-2070, for which a slight increase in spring is predicted. In autumn, in fact, the probability of low loadings state decreases gradually followed by an increase in the probability of high loadings which reach the 28% under the RCP8.5 2041-2070 (Figure 9c). These changes can be attribute to the predicted increase in runoff (Figure 8b) caused by increasing in precipitations in the autumn-winter period.

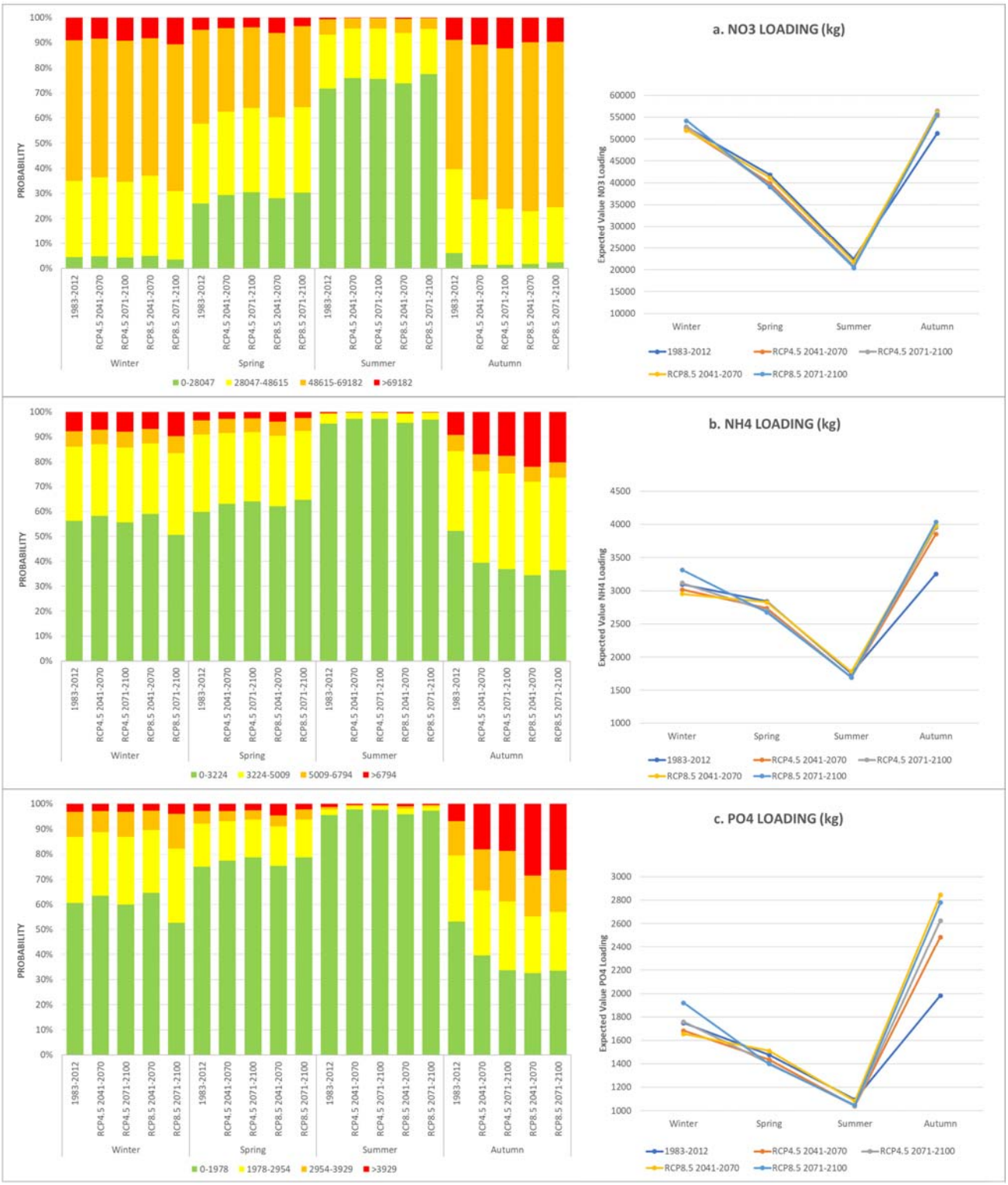


**Figure 9 Probabilistic (left) and deterministic (right) results for NO3- (a), NH4+ (b) and PO43- (c) loadings for different seasons across climate change scenarios**

Future nutrients loading scenarios developed through the BN, were also compared with those obtained using the SWAT model, forced with the same climate change scenarios (i.e. 1983-2012, 2041-2070, 2070-2100), in a previous analysis for the case study (for details see Pesce et al., (2018) (Table 1, Section 2.1)). Specifically, the percentage of instances where BN and SWAT simulations agreed on resulting outcome states resulted always more than 57% and 61% for $PO_4^{3-}$ and NH4 loadings respectively, while, for $NO_3^-$ loadings, the agreement was lower (i.e. between 58% and 44% depending on the scenarios). In general, the best agreement can be found for medium term periods (i.e. 2041-2070) (Figure V5, Annex V (SM)).

Figures 10 compares the Expected Value of the probability distributions of $PO_4^{3-}$ of SWAT simulation across different scenarios (blue) with BNs outputs (red) depicting a similar seasonal trend especially for medium term periods (Figure 9).

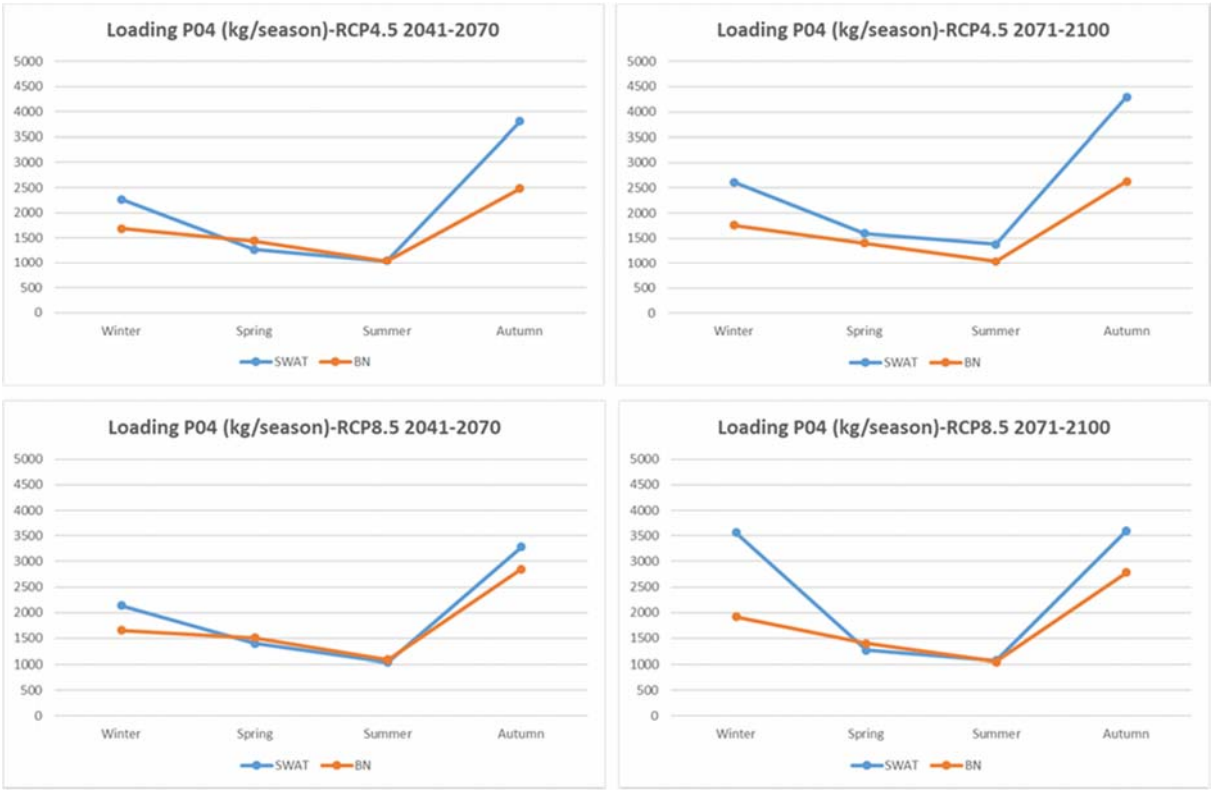


**Figure 10 Expected Value of the probability distributions of $PO_4^{3-}$ loading of SWAT model simulation across different scenarios (blue) and of Bayesian Network outputs (red), obtained by fixing the states of precipitation and temperature according with the same climate change projection.**

In general, major discrepancies between SWAT and BN simulation are found Winter and Autumn seasons (Figure 10, Figure V2 Annex V (SM), Figure V3 Annex V (SM)) for all the nutrients species.

SWAT and BN seasonal probability distributions are similar and characterized by comparable Variance and Standard Deviations (Figure V4, Annex V (SM)). While for $PO_4^{3-}$ and $NH_4^+$ SD is quite small, for $NO_3^-$ loadings and especially in autumn and winter distributions present a higher spread around their expected value denoting a higher uncertainty in the outcome respect to summer and spring.

## 4. Discussion

Scenarios obtained through BN simulations confirms that climate change will drive changes in both the hydrology and nutrient loadings as suggested by previous studies (Dunn et al., 2012; El-Khoury et al., 2015; Shrestha et al., 2017; Whitehead et al., 2009).Specifically, results indicate a high probability of an increase of freshwater discharge and nutrient loadings in autumn, and a slightly decrease in spring and summer with respect to the current conditions. Others Authors (Panagopoulos et al., 2011; and Bouraoui et al., 2002) reached similar conclusions analysing climate change and diffuse pollution effects at catchment level respectively in Greece and United Kingdom.

Climate change scenarios for the Zero river basin indicate that increase in temperatures combined with decreasing precipitation will increase evapotranspiration and consequently induce dry and low flow conditions in summer. These effects could be significantly greater than those experiences at the current conditions and could impact on the autumn hydrological responses of the basin.

Processes responsible for the reduced load in the summer season are mainly related with the increase of temperature which enhance the mineralization of organic matter during dry period followed then by the washing out of the accumulated nutrients during subsequent extreme precipitation events. This,

combined with reduced summer flow rates, could explain the increase loads in autumn months as suggested by others Authors (Whitehead et al., 2006 and Wilby et al., 2006).

Results also highlight that the processes governing nutrients losses from the basin to surface water under climate change scenarios are different depending on nutrients species. In fact, while $NO_3^-$ loadings resulted strongly dependent on river flow and temperature, runoff resulted the factors playing the greatest role in driving $NH_4^+$ loadings in the case study. In spring and summer, in fact, $NO_3^-$ and $NH_4^+$ are commonly applied as fertilizers amendments. In dry and warm conditions $NH_4^+$, however, is readily adsorbed to clay mineral and therefore is scarcely prone to movements. Its load is decreasing in summer and spring under projected climate change while increase, in autumn, drive up by runoff and extreme precipitation events. $N0_3$, on the other side, is highly soluble and thus suitable to be transported by hydrological flow (Lapp et al., 1998). In autumn, the elevated temperature and wet conditions projected will enhance nitrification process making $NO_3^-$ highly available. This, combined with the seasonal increase in the river flow, could explain the great increase of $NO_3^-$ load during autumn season respect to current scenarios. In the soil, soluble form of phosphorous ($PO_4^{3-}$) are mobile and can be transported by diffusion or by surface water flow. At elevated temperature and in dry condition, however, $PO_4^{3-}$ is easily adsorbed to clay particles or immobilized by organic matter accumulating in the upper soil layers (Lapp et al., 1998). This characteristic makes phosphorous available for transport to surface water, primarily by surface runoff (Weldehawaria, 2013). Accordingly, decrease of summer load can be attributed to the increase temperature and decrease precipitation enhancing $PO_4^{3-}$ immobilization and the reduction of sediment transport due to low flow conditions. In autumn, an increase in runoff, following the enrichment of the topsoil of phosphorous occurred during the summer, increase $PO_4^{3-}$ transport and thus its loads in the river. In addition, the projected increase of dry prolonged conditions in summer might speed up soil erosion phenomena and, consequently, enhance the runoff of adsorbed mineral forms of phosphorus

trough the basin leading to peak of $PO_4^{3-}$ load in autumn as soon as the drought breaks. Accordingly, strong relationships between phosphorous and the runoff magnitude have been reported by (Molina-Navarro et al., 2014; Shrestha et al., 2017) in Mediterranean catchments.

## Conclusions

The integrated assessment based on BNs proposed provides a mean to capture the dependencies between climate change and non-climatic drivers and their effect on water quality alterations. Simulated scenarios show that seasonal changes in precipitation and temperature are likely to modify both the hydrology and nutrient loadings of the Zero River. Both $NH_4^+$ and $PO_4^{3-}$ loadings are mainly influenced by changes in hydrological variables (i.e. runoff) while $NO_3^-$ loadings, despite being highly dependent on flow conditions, are also influenced by agronomic practices and land use (i.e. irrigation, fertilization). These findings confirm that climate change, will play a significant role in exacerbating the risk of water quality degradation especially considering that most dramatic changes (e.g. increase in precipitation and runoff) will happen during periods characterised by intensive agricultural activities (e.g. manure application in the fields during the autumn). Scenarios developed through the BN resulted to be consistent with observations from water quality monitoring stations and simulations produced by Pesce (2018) in the same case study area and for the same climate change scenarios using a hydrological model (i.e. SWAT).

However, discrepancies between observed and simulated scenarios exist especially for $NO_3^-$ loadings which is also the node characterized by highest level of uncertainty in the predicted outcomes in both baseline and future scenarios: this lack of fit suggest where improvements in model structure and accuracy of data collection should be oriented. Model performance, in fact, is strongly dependent on the quality and accuracy of data used for BN training. Our sensitivity analysis suggests that uncertainty in $NO_3^-$

loadings could be attributed to low quality of the information used to train nodes related with agronomic practices (i.e. fertilizer applications, irrigation), which are those mainly influencing $NO_3^-$ loadings. Due to data constraints, in fact, fertilizer application and irrigation have been considered uniform across the whole catchment while they both could vary considerably, both spatially and temporally, across the same season. Improving the accuracy of input data throughout the catchment and involving a higher number of experts in the model calibration would improve BN structure and its performance, reducing the uncertainty of future simulations.

In conclusion, the BN approach proposed was able to represent the effect of climate change and land use on water quality attributes in a policy-relevant manner, demonstrating the suitability of this method to supplement traditional process-based models (e.g. SWAT) commonly applied in water resources management, improving the treatment and communication of uncertainty and translating the information provided by deterministic analysis in a way which is directly usable and understandable also for non-expert users.

By identifying key components and processes affecting flow and water quality BNs could help in identifying knowledge gaps that need to be addressed, selecting variables of the system that should be targeted by adaptation strategies and the opportune typology of responses to implement. Being highly flexible, as new data and projections become available the developed BN can be easily revised updating evidences and uncertainty, thus increasing the robustness of the risk assessment outcomes (Failing et al., 2004), and contributing to the adaptive management process (Pollino and Henderson, 2010).

Finally, land use (i.e. agricultural land extension, crop typologies distribution) and agricultural management practices (i.e. amount of fertilizer application) changes, that in this BN version have been kept constant over future scenarios, should be accounted in future model improvements to provide a realist picture of future risks and allow their prioritization (Mantyka-Pringle et al., 2014). As this BN will

keep continuously updated, upcoming advances will overtake these current technical limitations. Moreover, further improvements of the proposed approach could consider the implementation of a dynamic version of the BN (Molina et al., 2013) to better handle temporal dynamics and the development of new scenarios, considering land use changes projections or assuming that specific management measures have been put in place.

**Acknowledgments:**

The research leading to these results has received funding from the Euro-Mediterranean Center on Climate Change (CMCC), Strategic Projects Funds (2016-2018). The authors would like to thank all the public authorities and local experts that provided territorial data and information supporting the implementation of the methodology, especially the Regional Agency for Environmental Protection and Prevention (ARPAV) and the Venice Water Authority. We also thank Monia Santini (CMCC) for providing the COSMO-CLM projections and Marco Pesce (Cà Foscari University) for making available the hydrological simulations for the Zero river basin. Finally, authors are grateful to the two anonymous reviewers for the supportive and constructive comments which helped in improving the final version of the manuscript.

**References**

Aguilera, P.A., Fernández, A., Fernández, R., Rumí, R., Salmerón, A., 2011. Bayesian networks in environmental modelling. Environ. Model. Softw. 26, 1376–1388.

Alam, M.J., Dutta, D., 2013. Predicting climate change impact on nutrient pollution in waterways: a case study in the upper catchment of the Latrobe River, Australia. Ecohydrology 6, 73–82.

Arnold, J.G., Moriasi, D.N., Gassman, P.W., Abbaspour, K.C., White, M.J., Srinivasan, R., Santhi, C., Harmel, R.D., Van Griensven, A., Van Liew, M.W., 2012. SWAT: Model use, calibration, and

validation. Trans. ASABE 55, 1491–1508.

Borsuk, M.E., Stow, C.A., Reckhow, K.H., 2004. A Bayesian network of eutrophication models for synthesis, prediction, and uncertainty analysis. Ecol. Modell. 173, 219–239.

Bouraoui, F., Galbiati, L., Bidoglio, G., 2002. Climate change impacts on nutrient loads in the Yorkshire Ouse catchment (UK). Hydrol. Earth Syst. Sci. Discuss. 6, 197–209.

Bromley, J., Jackson, N.A., Clymer, O.J., Giacomello, A.M., Jensen, F.V., 2005. The use of Hugin® to develop Bayesian networks as an aid to integrated water resource planning. Environ. Model. Softw. 20, 231–242.

Bucchignani, E., Montesarchio, M., Zollo, A.L., Mercogliano, P., 2016. High-resolution climate simulations with COSMO-CLM over Italy: performance evaluation and climate projections for the 21st century. Int. J. Climatol. 36, 735–756.

Burgman, M., 2005. Risks and decisions for conservation and environmental management. Cambridge University Press.

Bussi, G., Whitehead, P.G., Bowes, M.J., Read, D.S., Prudhomme, C., Dadson, S.J., 2016. Impacts of climate change, land-use change and phosphorus reduction on phytoplankton in the River Thames (UK). Sci. Total Environ. In review. doi:10.1016/j.scitotenv.2016.02.109

Carriger, J.F., Barron, M.G., Newman, M.C., 2016. Bayesian networks improve causal environmental assessments for evidence-based policy. Environ. Sci. Technol. 50, 13195–13205.

Catenacci, M., Giupponi, C., 2010. Potentials and limits of Bayesian networks to deal with uncertainty in the assessment of climate change adaptation policies.

Cattaneo, L., Zollo, A.L., Bucchignani, E., Montesarchio, M., Manzi, M.P., Mercogliano, P., 2012. Assessment of cosmo-clm performances over mediterranean area.

Coupé, V.M.H., Peek, N., Ottenkamp, J., Habbema, J.D.F., 1999. Using sensitivity analysis for efficient quantification of a belief network. Artif. Intell. Med. 17, 223–247.

Culbertson, A.M., Martin, J.F., Aloysius, N., Ludsin, S.A., 2016. Anticipated impacts of climate change on 21st century Maumee River discharge and nutrient loads. J. Great Lakes Res. 42, 1332–1342.

CVN, 2006. Regime Degli Apporti Di Acqua Dolce in Laguna Di Venezia.

de Santa Olalla, F.J.M., Domínguez, A., Artigao, A., Fabeiro, C., Ortega, J.F., 2005. Integrated water resources management of the hydrogeological unit “Eastern Mancha” using Bayesian belief networks. Agric. Water Manag. 77, 21–36.

Dunn, S.M., Brown, I., Sample, J., Post, H., 2012. Relationships between climate, water resources, land use and diffuse pollution and the significance of uncertainty in climate change. J. Hydrol. 434, 19–35.

EEA, 1999. Environmental indicators : Typology and overview. Eur. Environ. Agency 25, 19.

Eghball, B., Wienhold, B.J., Gilley, J.E., Eigenberg, R.A., 2002. Mineralization of manure nutrients. J. Soil Water Conserv. 57, 470–473.

El-Khoury, A., Seidou, O., Lapen, D.R., Que, Z., Mohammadian, M., Sunohara, M., Bahram, D., 2015. Combined impacts of future climate and land use changes on discharge, nitrogen and phosphorus loads for a Canadian river basin. J. Environ. Manage. 151, 76–86.

Facca, C., Ceoldo, S., Pellegrino, N., Sfriso, A., 2014. Natural recovery and planned intervention in coastal wetlands: Venice Lagoon (Northern Adriatic Sea, Italy) as a case study. Sci. World J. 2014.

Failing, L., Horn, G., Higgins, P., 2004. Using expert judgment and stakeholder values to evaluate adaptive management options. Ecol. Soc. 9, 13.

Franco, C., Hepburn, L.A., Smith, D.J., Nimrod, S., Tucker, A., 2016. A Bayesian Belief Network to assess rate of changes in coral reef ecosystems. Environ. Model. Softw. 80, 132–142.

Hand, D.J., 1997. Construction and assessment of classification rules. Wiley Chichester.

Huttunen, I., Lehtonen, H., Huttunen, M., Piirainen, V., Korppoo, M., Veijalainen, N., Viitasalo, M., Vehviläinen, B., 2015. Effects of climate change and agricultural adaptation on nutrient loading from Finnish catchments to the Baltic Sea. Sci. Total Environ. 529, 168–181. doi:10.1016/j.scitotenv.2015.05.055

Interne, S.A., 2008. Servizio Acque Interne. 2008. Le Acque Sotterranee Della Pianura Veneta - I Risultati Del Progetto SAMPAS. Technical Report. Padova, PD, Italy.

IPCC, 2013. WORKING GROUP I CONTRIBUTION TO THE IPCC FIFTH ASSESSMENT REPORT CLIMATE CHANGE 2013 : THE PHYSICAL SCIENCE BASIS Final Draft Underlying Scientific-Technical

Assessment A report accepted by Working Group I of the IPCC but not approved in detail . Chapter 13.

Jiménez Cisneros, B.E., Fischer, T., Barros, R., Dokken, D., Mach, K., Bilir, T., Chatterjee, M., Ebi, K., Estrada, Y., Genova, R., Girma, B., Kissel, E., Levy, A., MacCracken, S., 2014. 3 Freshwater Resources Coordinating Lead Authors: Contributing Authors. Shinjiro Kanae (Japan) 229–269.

Kragt, M.E., 2009. A beginners guide to Bayesian network modelling for integrated catchment management. Landscape Logic.

Kristensen, P., 2004. The DPSIR framework. A Compr. / Detail. Assess. vulnerability water Resour. to Environ. Chang. Africa using river basin approach. 1–10.

Landis, W.G., Durda, J.L., Brooks, M.L., Chapman, P.M., Menzie, C.A., Stahl, R.G., Stauber, J.L., 2013. Ecological risk assessment in the context of global climate change. Environ. Toxicol. Chem. 32, 79–92.

Landuyt, D., Broekx, S., D'hondt, R., Engelen, G., Aertsens, J., Goethals, P.L.M., 2013. A review of Bayesian belief networks in ecosystem service modelling. Environ. Model. Softw. 46, 1–11.

Lapp, P., Madramootoo, C.A., Enright, P., Papineau, F., Perrone, J., 1998. WATER QUALITY OF AN INTENSWE AGRICULTURAL WATERSHED IN QUEBEC. JAWRA J. Am. Water Resour. Assoc. 34, 427–437.

Lu, Q., Johnson, A.C., Jürgens, M.D., Sweetman, A., Jin, L., Whitehead, P., 2015. The distribution of Polychlorinated Biphenyls (PCBs) in the River Thames Catchment under the scenarios of climate change. Sci. Total Environ. 533, 187–95. doi:10.1016/j.scitotenv.2015.06.084

Lundekvam, H.E., Romstad, E., Øygarden, L., 2003. Agricultural policies in Norway and effects on soil erosion. Environ. Sci. Policy 6, 57–67.

Madsen, A.L., Jensen, F., Kjaerulff, U.B., Lang, M., 2005. The Hugin tool for probabilistic graphical models. Int. J. Artif. Intell. Tools 14, 507–543.

Mantyka-Pringle, C.S., Martin, T.G., Moffatt, D.B., Linke, S., Rhodes, J.R., 2014. Understanding and predicting the combined effects of climate change and land-use change on freshwater macroinvertebrates and fish. J. Appl. Ecol. 51, 572–581.

Marcos-Garcia, P., Lopez-Nicolas, A., Pulido-Velazquez, M., 2017. Combined use of relative drought indices to analyze climate change impact on meteorological and hydrological droughts in a Mediterranean basin. J. Hydrol.

Marcot, B.G., 2012. Metrics for evaluating performance and uncertainty of Bayesian network models. Ecol. Modell. 230, 50–62.

McCann, R.K., Marcot, B.G., Ellis, R., 2006. Bayesian belief networks: applications in ecology and natural resource management. Can. J. For. Res. 36, 3053–3062.

Molina-Navarro, E., Trolle, D., Martínez-Pérez, S., Sastre-Merlín, A., Jeppesen, E., 2014. Hydrological and water quality impact assessment of a Mediterranean limno-reservoir under climate change and land use management scenarios. J. Hydrol. 509, 354–366.

Molina, J.-L., Pulido-Velázquez, D., García-Aróstegui, J.L., Pulido-Velázquez, M., 2013. Dynamic Bayesian networks as a decision support tool for assessing climate change impacts on highly stressed groundwater systems. J. Hydrol. 479, 113–129.

Molina, J.-L., Zazo, S., Rodríguez-Gonzálvez, P., González-Aguilera, D., 2016. Innovative Analysis of Runoff Temporal Behavior through Bayesian Networks. Water 8, 484.

Newton, A.C., 2009. Bayesian Belief Networks in environmental modelling: a review of recent progress. Environ. Model. Res. Nov. Sci. Publ. Hauppauge, New York, USA 13–50.

Nielsen, T.D., Jensen, F.V., 2009. Bayesian networks and decision graphs. Springer Science & Business Media.

O'Hagan, A., 2012. Probabilistic uncertainty specification: Overview, elaboration techniques and their application to a mechanistic model of carbon flux. Environ. Model. Softw. 36, 35–48.

Ockenden, M.C., Deasy, C.E., Benskin, C.M.H., Beven, K.J., Burke, S., Collins, A.L., Evans, R., Falloon, P.D., Forber, K.J., Hiscock, K.M., 2016. Changing climate and nutrient transfers: Evidence from high temporal resolution concentration-flow dynamics in headwater catchments. Sci. Total Environ. 548, 325–339.

Panagopoulos, Y., Makropoulos, C., Mimikou, M., 2011. Diffuse surface water pollution: driving factors for different geoclimatic regions. Water Resour. Manag. 25, 3635.

Pearl, J., 1988. Probabilistic reasoning in intelligent systems: networks of plausible inference. Morgan Kaufmann.

Pesce, M., Critto, A., Torresan, S., Giubilato, E., Santini, M., Zirino, A., Ouyang, W., Marcomini, A., 2018. Modelling climate change impacts on nutrients and primary production in coastal waters. Sci. Total Environ. 628, 919–937.

Phan, T.D., Smart, J.C.R., Capon, S.J., Hadwen, W.L., Sahin, O., 2016. Applications of Bayesian belief networks in water resource management: A systematic review. Environ. Model. Softw. 85, 98–111.

Pollino, C.A., Henderson, C., 2010. Bayesian networks: A guide for their application in natural resource management and policy. Landsc. Logic, Tech. Rep. 14.

Pollino, C.A., Woodberry, O., Nicholson, A., Korb, K., Hart, B.T., 2007. Parameterisation and evaluation of a Bayesian network for use in an ecological risk assessment. Environ. Model. Softw. 22, 1140–1152.

Power, M., McCarty, L.S., 2006. Environmental risk management decision-making in a societal context. Hum. Ecol. Risk Assess. 12, 18–27.

Pulido-Velazquez, M., Peña-Haro, S., García-Prats, A., Mocholi-Almudever, A.F., Henriquez-Dole, L., Macian-Sorribes, H., Lopez-Nicolas, A., 2015. Integrated assessment of the impact of climate and land use changes on groundwater quantity and quality in the Mancha Oriental system (Spain). Hydrol. Earth Syst. Sci. 19, 1677–1693.

Riahi, K., Rao, S., Krey, V., Cho, C., Chirkov, V., Fischer, G., 2011. RCP 8 . 5 — A scenario of comparatively high greenhouse gas emissions 33–57. doi:10.1007/s10584-011-0149-y

Rockel, B., Will, A., Hense, A., 2008. The regional climate model COSMO-CLM (CCLM). Meteorol. Zeitschrift 17, 347–348.

Ronco, P., Zennaro, F., Torresan, S., Critto, A., Santini, M., Trabucco, A., Zollo, A.L., Galluccio, G., Marcomini, A., 2017. A risk assessment framework for irrigated agriculture under climate change. Adv. Water Resour.

Scoccimarro, E., Gualdi, S., Bellucci, A., Sanna, A., Fogli, P.G., Manzini, E., Vichi, M., Oddo, P., Navarra, A., 2011. Effects of Tropical Cyclones on Ocean Heat Transport in a High-Resolution Coupled General Circulation Model. J. Clim. 24, 4368–4384. doi:10.1175/2011JCLI4104.1

Shrestha, M.K., Recknagel, F., Frizenschaf, J., Meyer, W., 2017. Future climate and land uses effects on flow and nutrient loads of a Mediterranean catchment in South Australia. Sci. Total Environ. 590, 186–193.

Sperotto, A., Molina, J.-L., Torresan, S., Critto, A., Marcomini, A., 2017. Reviewing Bayesian Networks potentials for climate change impacts assessment and management: A multi-risk perspective. J. Environ. Manage. 202, 320–331.

Stelzenmüller, V., Lee, J., Garnacho, E., Rogers, S.I., 2010. Assessment of a Bayesian Belief Network–GIS framework as a practical tool to support marine planning. Mar. Pollut. Bull. 60, 1743–1754.

Terzi, S., Torresan, S., Schneiderbauer, S., Critto, A., Zebisch, M., Marcomini, A., 2019. Multi-risk assessment in mountain regions: A review of modelling approaches for climate change adaptation. J. Environ. Manage. 232, 759–771.

Thomson, A.M., Calvin, K. V, Smith, S.J., Kyle, G.P., Volke, A., Patel, P., Delgado-Arias, S., Bond-Lamberty, B., Wise, M.A., Clarke, L.E., 2011. RCP4. 5: a pathway for stabilization of radiative forcing by 2100. Clim. Change 109, 77.

Venezia, O. naturalistico della L. del C. di, Guerzoni, S., 2006. Atlante della laguna: Venezia tra terra e mare. Marsilio.

Weldehawaria, S.S., 2013. Monitoring Runoff Chemistry into the Vansjø Basin with Focus on the Role of Particles and DNOM in the Transport of Nutrients.

Whitehead, P., Butterfield, D., Wade, D., 2008. Potential impacts of climate change on river water quality.

Whitehead, P.G., Wilby, R.L., Battarbee, R.W., Kernan, M., Wade, A.J., 2009. A review of the potential impacts of climate change on surface water quality. Hydrol. Sci. J. 54, 101–123.

Whitehead, P.G., Wilby, R.L., Butterfield, D., Wade, A.J., 2006. Impacts of climate change on in-stream nitrogen in a lowland chalk stream: an appraisal of adaptation strategies. Sci. Total Environ. 365, 260–273.

Wilby, R.L., Whitehead, P.G., Wade, A.J., Butterfield, D., Davis, R.J., Watts, G., 2006. Integrated modelling of climate change impacts on water resources and quality in a lowland catchment: River Kennet, UK. J. Hydrol. 330, 204–220.

Zabel, F., 2016. Impact of Climate Change on Water Availability, in: Regional Assessment of Global Change Impacts. Springer, pp. 463–469.

Zuliani, A., Zaggia, L., Collavini, F., Zonta, R., 2005. Freshwater discharge from the drainage basin to the Venice Lagoon (Italy). Environ. Int. 31, 929–938.

## Annex I-Information and assumptions used to calculate node's states and probabilities in the BN

Annex I provides an extensive description of the information and assumptions used to characterize states, prior and conditional probabilities of nodes in the BN developed for the Zero river basin (Figure 3). As described in Section 2.2.2, for most nodes, prior probability and conditional probability distributions have been extrapolated directly from the frequencies of observations or simulations available for the corresponding variables. For other nodes, they have been calculated as follows.

### N and P fertilizer application

Nodes related with the nitrogen and phosphorous fertilizer application, describe respectively the amount (kg/ha) of P and N fertilizers applied for each season according to different crop typology.

Accordingly, their parametrization was based on the seasonal needs of N and P for the three main crops of the case study (i.e. Corn, Soy, Winter Wheat) (Table 1I). This information was obtained from both literature (Carpani and Giupponi, 2010) and interviews with experts of Veneto Agricoltura (Bonetto, 2012; Regione Veneto, 2014).

**Table I1 Seasonal amount of N and P fertilizers (kg/ha) applied to different crop typologies in the case study**

| Fertilizer application (kg/ha) | | Winter | Spring | Summer | Autumn |
|---|---|---|---|---|---|
| **Corn** | N | 0 | 50 | 230 | 0 |
| | P | 0 | 120 | 0 | 0 |
| **Winter Wheat** | N | 50 | 100 | 0 | 30 |
| | P | 0 | 0 | 0 | 100 |
| **Soy** | N | 0 | 30 | 0 | 0 |
| | P | 0 | 100 | 0 | 0 |

### Water needs

The node "Water needs" represent the depth (mm) of water needed from different crop s to meet the water loss through evapotranspiration and thus the amount of water needed to grow optimally. Accordingly, node states and probabilities have been calculated based on the empirical Equation I.I proposed by FAO ((Brouwer and Heibloem, 1986) :

$$\textbf{Water Needs}_{crop} = Et_p \times K_c \qquad \textit{Equation I.I}$$

**where:**

Water Needs $_{crop}$ is the crop water needs (mm/season);
$K_c$ is the crop factor;
$Et_p$ is the reference evapotranspiration (mm/season).

The Kc for the three types of crops, incorporating crop characteristics and effects of evaporation from the soil, have been selected according with FAO (Allen et al., 1998) (Table I2).

**Table I2 Kc for different crop typologies in the case study**

| Kc | Winter | Spring | Summer | Autumn |
|---|---|---|---|---|
| **Corn** | 0 | 0.3 | 1.2 | 0.6 |
| **Winter Wheat** | 1.15 | 0.25 | 0 | 0.7 |
| **Soy** | 0 | 0.4 | 1 | 0.5 |

**Irrigation**

The node "Irrigation" represents the amount of water applied as artificial irrigation (mm) for each season and, in the BN, it is directly dependent on the water needs and the effective rainfall (i.e. the amount of precipitation that is stored in the soil and thus available for the plant). Accordingly, its probability distribution has been calculated based on Equation I.II (Brouwer and Heibloem, 1986):

**Irrigation = Water needs $_{crop}$-ER** ***Equation I.II***

**where:**

Irrigation is the amount of water applied as irrigation (mm/season);
Water Needs $_{crop}$ is the crop water needs (mm/season);
ER is the effective rainfall (mm/season).

**Total N and P loadings**

The nodes "Total N loadings" and "Total P loadings represent the total amount of N and P that are discharged from the river basin into the river seasonally. They are the results of the sum of the loadings apportioned to point and non-point sources and, accordingly, their probability distributions were calculated based on Equation I.III (here presented for N):

**N total loading= N point sources+ N diffuse sources** ***Equation I.III***

**where:**

N total loading is the loading of nitrogen in the river (kg/season);
N point sources is the amount of nitrogen coming from point sources (i.e. WWTPs and Industrial discharges) (kg/season);
N diffuse sources is the amount of nitrogen coming from agricultural practices (kg/seasons)

## Annex II-Bayesian Network Configurations

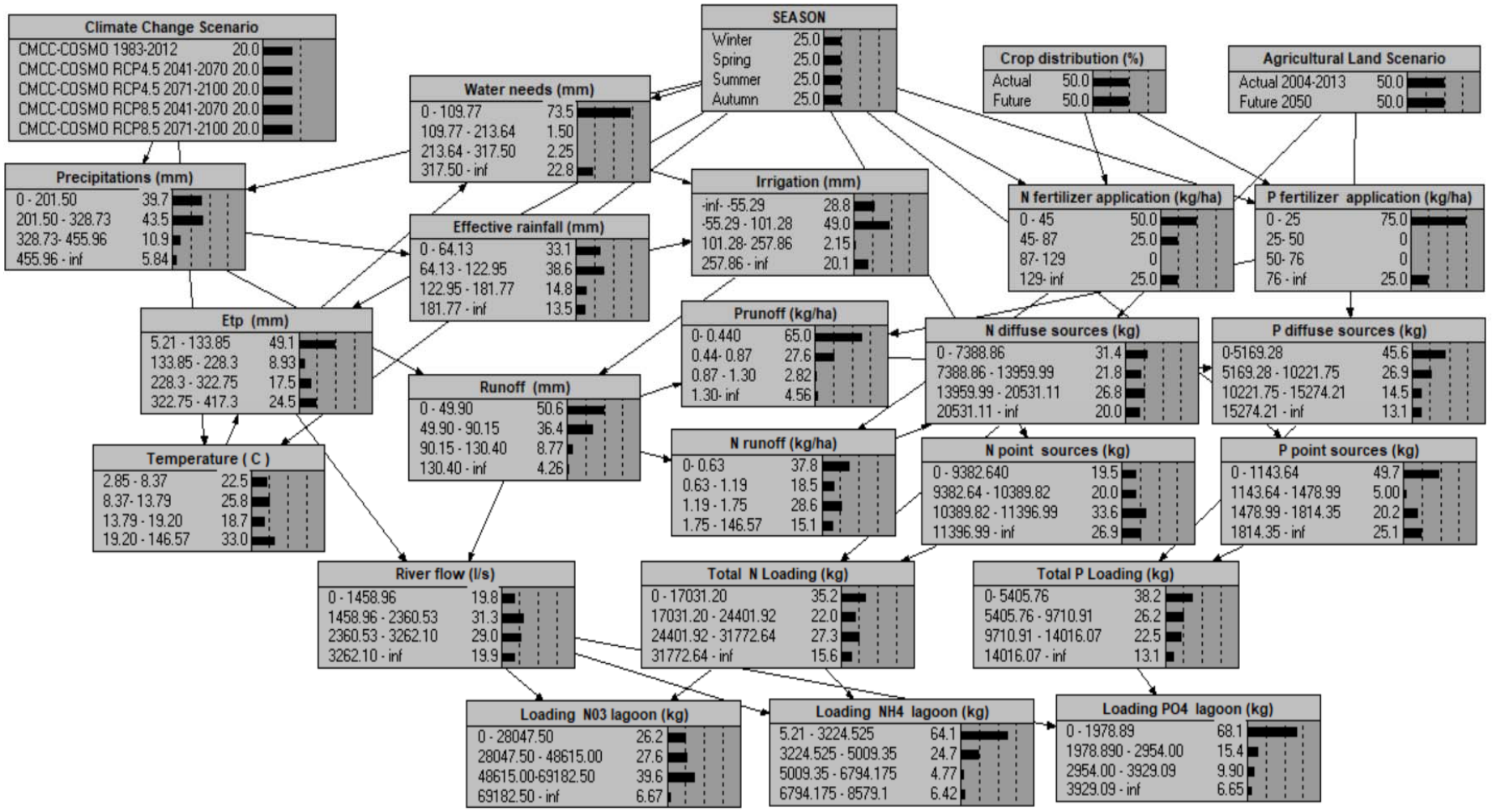


**Figure II1 Configuration of the Bayesian Network for the Zero river basin trained with the information for the period 2004-2013**

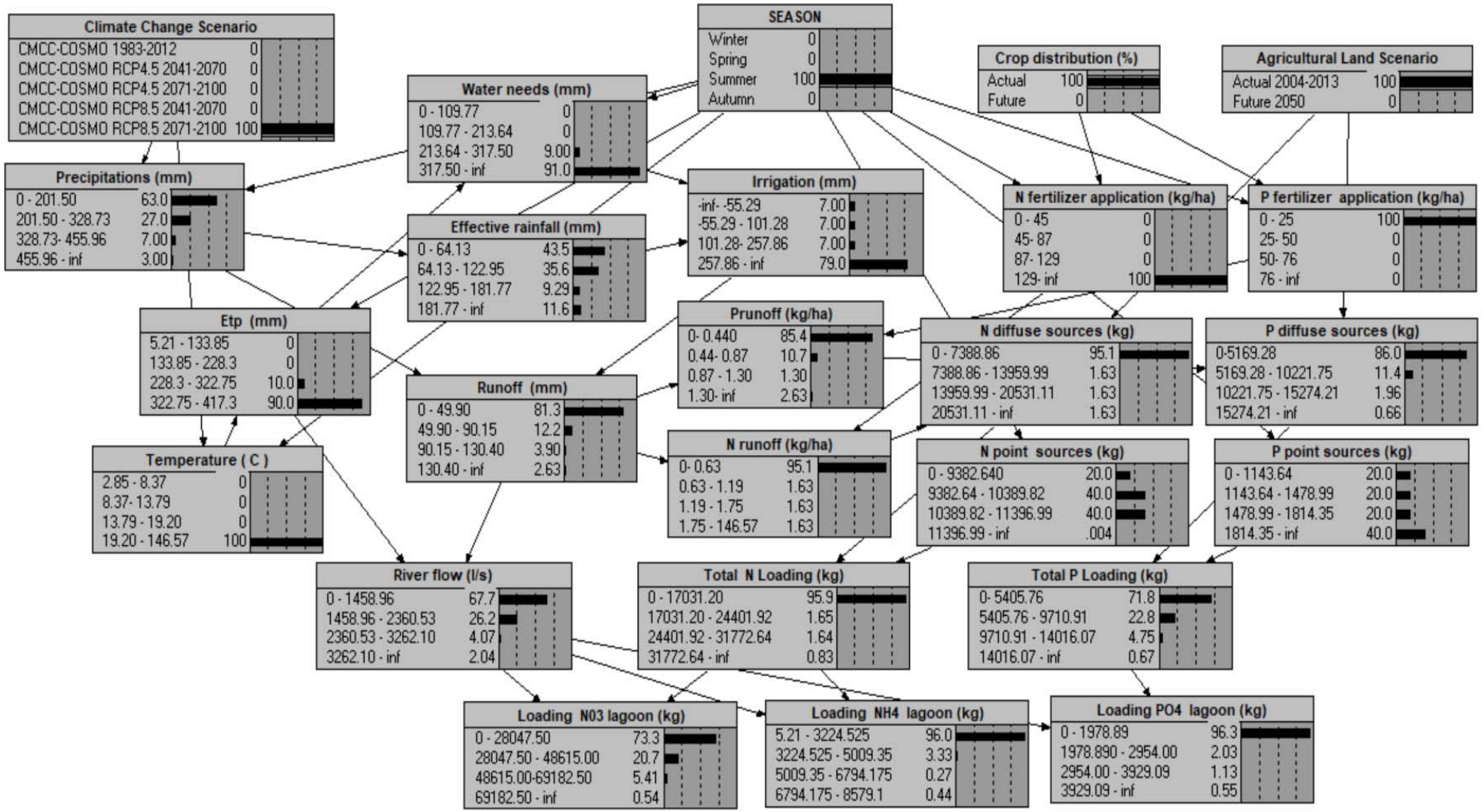


**Figure II2 Configuration of the BN for the Zero river basin used for scenario analyisis simulating the nutrients loadings (kg/season) under the COSMO-CLM RCP8.5 2071-2100 climate change scenarios and current land use in summer season**

## Annex III- Expected Value of the Probability distribution

The Expected Value of the probability distribution of a discrete random variable represents the probability-weighted average of all possible values the variable can assume. In other words, each possible value of random is multiplied by its probability of occurring, and the resulting products are summed to produce the expected value. For a finite discrete random variable *X* the Expected Value E(X) is defined as (Equation III.I):

**E(X)= x1****p1*** **+ x2****p2*** **+ ----- + xk****pk*** ***Equation III.I***

**where:**

E(X) is the expected value of X;

x1,x2,…,xk are the finite number of outcomes of X;

*p1, p2,…,pk* are the probabilities associated to each outcome of X.

Within the BN developed for the case of study, however each variable is characterized by multiple states (i.e. intervals) and therefore the Expected Value has been calculated as the sum of the products of the intermediate value of each interval/state of the variable for its associated probability (Equation III.II):

**E(X)= I1****p1*** **+ I2****p2*** **+ ----- + Ik****pk*** ***Equation III.II***

**where:**

E(X) is the expected value of X;

I1,I2,…,Ik are the intermediate value of each interval/state of X;

*p1, p2,…,pk* are the probabilities associated to each intermediate value of each interval of X.

Table III1 provide an example of the application of Equation II.II for the calculus of the Expected Value for the variable “Loading NO3 in the lagoon” of the BN.

**E (Loading NO3) =** 14023.67**0.05* + 38331.25**0.32*+ 58898.75*0.55 + 83206.25*0.08 **=** 52284.6

**Table III1 Example of the computation on the Expected Value for the variable "Loading $NO_3$ in the lagoon"**

| Variable (X) | Interval/State | Probabilities (p) | Intermediate value (I) |
|---|---|---|---|
| Loading NO3 in the lagoon | 0-28047 | 0.05 | 14023.75 |
| | 28047-48615 | 0.32 | 38331.25 |
| | 48615-69182 | 0.55 | 58898.75 |
| | 69182-97230 | 0.08 | 83206.25 |

## Annex IV Percent change

The Percent change is a measure of the change of a variable intensity, magnitude or extent over time. In this case, it is used to measure the increase or decrease of the Expected value of output nodes as consequence of the maximization of input nodes according with Equation V.I

$$\textbf{Percent change}=\left(\left(\frac{New\ Expected\ Value}{Expect\ Value}\right)-100\right)*100 \qquad \textit{Equation IV.I}$$

**where:**

New Expected Value is the Expected Value of the output node after the maximization of input nodes;
Expected Value is the initial Expected Value of the output node.

Results of the application of Equation V.I to all the nodes of the BN are provided in Table V1.

**Table IV1 Percentage change (%) of output variables (i.e. $NO_3$, $NH_4$, $PO_4$ loadings)**

| | Temperature | Precipitation | Etp | Water Needs | Irrigation | Effective rainfall | Runoff | Flow | Nrunoff | Prunoff | Nfertilizerapp | Pfertilizer app | Ndiffuse sources | Pdiffuse sources | Npoint sources | Ppoint sources | TotalN | TotalP |
|---|---|---|---|---|---|---|---|---|---|---|---|---|---|---|---|---|---|---|
| **NO3** | 37.0 | 29.1 | 49.2 | 50.0 | 51.7 | 13.2 | 31.2 | 47.6 | 32.6 | 0.0 | 46.3 | 0.0 | 32.6 | 0.0 | 21.7 | 0.0 | 38.1 | 0.0 |
| **NH4** | 28.6 | 57.6 | 38.1 | 38.3 | 39.8 | 24.2 | 76.4 | 71.1 | 0.5 | 0.0 | 36.1 | 0.0 | 0.1 | 0.0 | 18.1 | 0.0 | 9.5 | 0.0 |
| **PO4** | 27.6 | 92.9 | 35.0 | 35.0 | 37.4 | 38.9 | 111.6 | 54.5 | 0.0 | 102.0 | 0.0 | 11.2 | 0.0 | 100.1 | 0.0 | 10.8 | 0.0 | 100.0 |

## Annex V-Evaluation results

| | Winter | Spring | Summer | Autumn | Total |
|---|---|---|---|---|---|
| Loading NO3 | 1.04 | 1.18 | 0.76 | 0.97 | 1.24 |
| Loading NH4 | 1.09 | 0.92 | 0.2 | 1.18 | 0.98 |
| Loading PO4 | 1.08 | 0.74 | 0.22 | 1.26 | 0.97 |

**Figure V1 Uncertainty analysis showing seasonal and total entropy values for different BN output nodes**


**Figure V2 Expected Value of the probability distributions of $NO_3$ loading of SWAT model simulation across different scenarios (blue) and of Bayesian Network outputs (red), obtained by fixing the states of precipitation and temperature according with the same climate change projection**

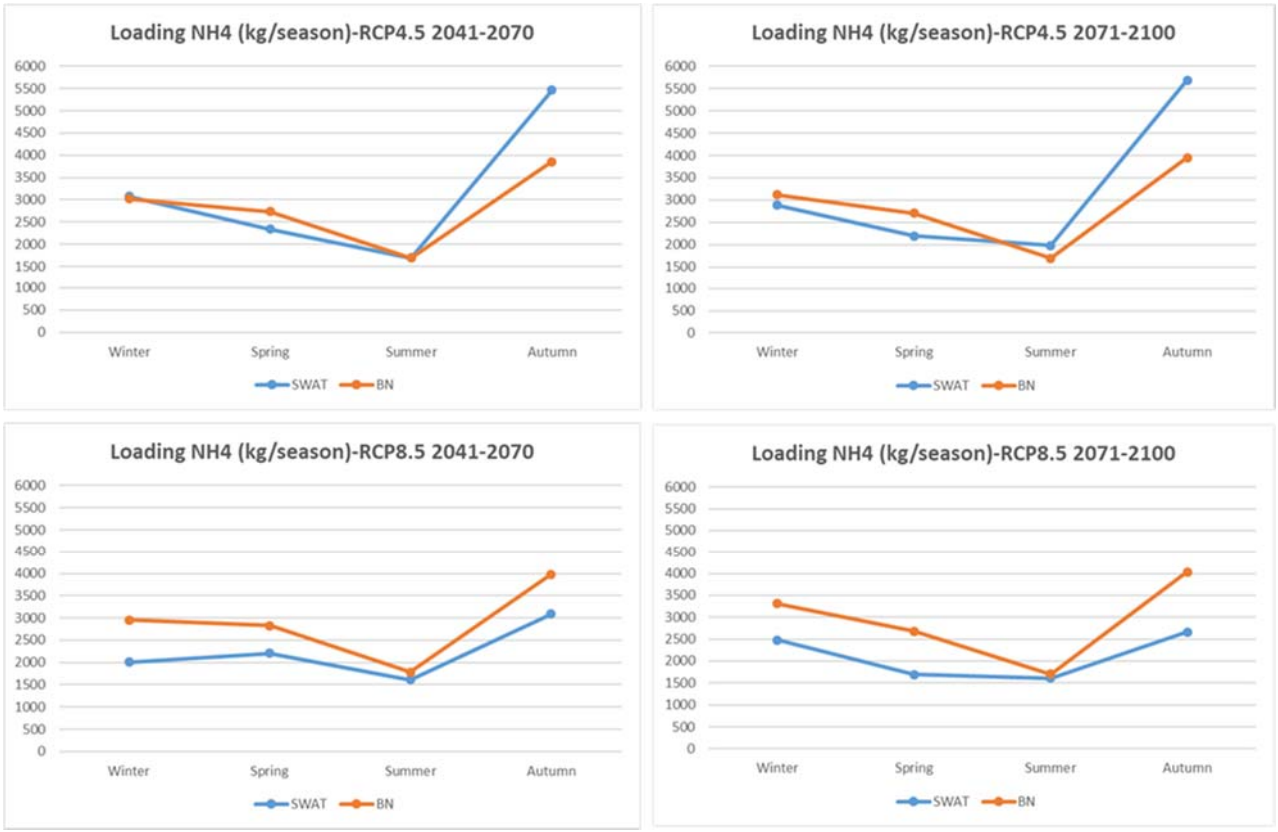


**Figure V3 Expected Value of the probability distributions of $NH_4$ loading of SWAT model simulation across different scenarios (blue) and of Bayesian Network outputs (red), obtained by fixing the states of precipitation and temperature according with the same climate change projection.**

| | | | | Winter | Spring | Summer | Autumn |
|---|---|---|---|---|---|---|---|
| PO4 | RCP4.5 2041-2070 | BN | μ | 1682.0 | 1435.4 | 1039.5 | 2484.5 |
| | | | SD | 1438.6 | 1323.5 | 1053.1 | 1840.8 |
| | | SWAT | μ | 2266.6 | 1268.1 | 1038.7 | 3804.8 |
| | | | SD | 1802.4 | 1184.1 | 1007.1 | 1724.4 |
| | RCP4.5 2071-2100 | BN | μ | 1758.5 | 1403.6 | 1040.5 | 2624.6 |
| | | | SD | 1490.4 | 1300.3 | 1054.4 | 1921.2 |
| | | SWAT | μ | 2610.3 | 1596.0 | 1382.4 | 4296.1 |
| | | | SD | 1800.6 | 1271.8 | 1460.0 | 1109.0 |
| | RCP8.5 2041-2070 | BN | μ | 1654.5 | 1510.6 | 1083.1 | 2844.0 |
| | | | SD | 1414.4 | 1391.5 | 1110.9 | 1867.5 |
| | | SWAT | μ | 2136.6 | 1399.1 | 1038.7 | 3281.9 |
| | | | SD | 1462.5 | 1325.0 | 1007.1 | 1651.8 |
| | RCP8.5 2071-2100 | BN | μ | 1920.7 | 1398.8 | 1046.9 | 2779.1 |
| | | | SD | 1609.1 | 1298.6 | 1062.5 | 1876.0 |
| | | SWAT | μ | 3559.6 | 1268.1 | 1071.2 | 3592.1 |
| | | | SD | 1895.4 | 1198.4 | 1158.1 | 1889.6 |
| NH4 | RCP4.5 2041-2070 | BN | μ | 3017.1 | 2737.6 | 1691.4 | 3856.2 |
| | | | SD | 2336.2 | 2193.6 | 1672.2 | 2425.8 |
| | | SWAT | μ | 3078.6 | 2339.7 | 1695.8 | 5460.3 |
| | | | SD | 2741.3 | 1950.5 | 1645.6 | 2595.5 |
| | RCP4.5 2071-2100 | BN | μ | 3119.0 | 2704.3 | 1692.5 | 3953.6 |
| | | | SD | 2360.7 | 2185.3 | 1672.6 | 2445.7 |
| | | SWAT | μ | 2887.6 | 2196.7 | 1981.7 | 5686.8 |
| | | | SD | 2420.0 | 1689.2 | 2194.0 | 3101.7 |
| | RCP8.5 2041-2070 | BN | μ | 2955.0 | 2830.0 | 1782.0 | 3976.0 |
| | | | SD | 2337.6 | 2225.7 | 1712.5 | 2457.0 |
| | | SWAT | μ | 2005.7 | 2208.2 | 1612.3 | 3090.1 |
| | | | SD | 1964.6 | 2166.1 | 1612.3 | 2158.2 |
| | RCP8.5 2071-2100 | BN | μ | 3314.1 | 2677.6 | 1698.0 | 4034.8 |
| | | | SD | 2394.9 | 2164.1 | 1675.2 | 2411.9 |
| | | SWAT | μ | 2482.7 | 1695.8 | 1612.3 | 2661.1 |
| | | | SD | 2182.8 | 1645.6 | 1612.3 | 2549.0 |
| NO3 | RCP4.5 2041-2070 | BN | μ | 52284.6 | 39945.3 | 20861.2 | 55511.5 |
| | | | SD | 45422.4 | 35949.9 | 19025.5 | 47968.6 |
| | | SWAT | μ | 76724.3 | 48615.0 | 14834.0 | 52292.3 |
| | | | SD | 30917.4 | 40520.9 | 14440.0 | 43681.7 |
| | RCP4.5 2071-2100 | BN | μ | 52981.4 | 39283.1 | 20946.1 | 56615.1 |
| | | | SD | 45896.6 | 35293.3 | 19076.4 | 48773.6 |
| | | SWAT | μ | 79965.3 | 53227.2 | 16454.5 | 56094.2 |
| | | | SD | 21717.3 | 39321.7 | 14995.3 | 44296.6 |
| | RCP8.5 2041-2070 | BN | μ | 52074.1 | 41172.9 | 21803.7 | 56176.7 |
| | | | SD | 45254.3 | 36474.0 | 20376.6 | 49709.5 |
| | | SWAT | μ | 65505.4 | 38518.2 | 14834.0 | 38642.8 |
| | | | SD | 49307.9 | 24585.0 | 14440.0 | 21960.9 |
| | RCP8.5 2071-2100 | BN | μ | 54281.0 | 39127.7 | 20509.7 | 55642.9 |
| | | | SD | 46833.4 | 35271.9 | 19184.6 | 49243.5 |
| | | SWAT | μ | 72922.3 | 41260.5 | 14023.8 | 38268.8 |
| | | | SD | 34459.5 | 31954.3 | 14023.8 | 29133.8 |

**Figure V4 Expected Value (μ) and Standard Deviation (SD) of the probability distributions of SWAT and BN simulation across different scenarios.**

| Loading PO4 | | | |
|---|---|---|---|
| RCP 4.5 2041-2070 | 68.3 | RCP 8.5 2041-2070 | 70.0 |
| RCP 4.5 2071-2100 | 60.0 | RCP 8.5 2071-2100 | 56.7 |
| Loading NH4 | | | |
| RCP 4.5 2041-2070 | 82.5 | RCP 8.5 2041-2070 | 70.0 |
| RCP 4.5 2071-2100 | 75.8 | RCP 8.5 2071-2100 | 60.8 |
| Loading NO3 | | | |
| RCP 4.5 2041-2070 | 58.3 | RCP 8.5 2041-2070 | 56.7 |
| RCP 4.5 2071-2100 | 49.2 | RCP 8.5 2071-2100 | 44.1 |

**Figure V5 Percentages (%) of instance where SWAT and BN simulations agree on predicted states for different outputs nodes**

## Annex VI-Detail description of the assessmen of COSMO-CLM performances

An assessment of COSMO-CLM performances for historical simulations has been carried out for the period 1973-2000 using different set of independent observed data as extensively described in (Bucchignani et al., 2016; Cattaneo et al., 2012).
First, a model evaluation for the whole Italian domain was performed using the E-OBS dataset (Haylock et al., 2008), an European daily high-resolution (0.25°) gridded dataset for precipitation and temperature covering the period 1950–2012 and representing a valuable standard reference dataset for climate research and is widely used for RCM evaluation over Europe. Despite providing huge advantages in term of spatial and temporal coverage, this dataset is affected by a number of potential inaccuracies: typical errors include incorrect station location and inhomogeneities in the station time series. Accordingly, additional high-resolution datasets were also considered in order to perform more accurate validation in the north-east part of the Italian domain (where case study area is located) including the gridded EURO4M-APGD dataset (Isotta et al., 2014) covering Northern Italy (resolution 5 km, daily time resolution, period 1971–2008) and a collections of precipitation station data provided by regional ARPAs and by the Civil Protection for the Veneto region (period 1980–2000).
Integrated results considering all the aforementioned observational dataset agree in confirming that COSMO-CLM simulations allow a satisfactory representation of the Italian climate with biases being lower than values that affect 'state-of-the-art' regional climate simulations (i.e. EURO-CORDEX data at 0.11°) with a high detail level.
Specifically, values of mean temperature show a general good agreement with observations: seasonal evaluation against E-OBS displays a negative bias in winter and a positive one in summer. However, comparison with regional datasets confirmed that part of the bias might be due to the low quality of E-OBS and furthermore it was shown that the resolution increase produces a good bias reduction.
With regard to precipitation, the model highlighted good agreement with accurate regional datasets, but improvements with a resolution increase are visible only in some areas.
For more details about the validation procedure and results please refer to Bucchignani et al. (2016) and Cattaneo et al. (2012).

### References:


Allen, R.G., Pereira, L.S., Raes, D., Smith, M., 1998. Crop evapotranspiration-Guidelines for computing crop water requirements-FAO Irrigation and drainage paper 56. FAO, Rome 300, D05109.

Bonetto, C. and L.F., 2012. Gestione Fertilizzanti E Contributi Tecnici Sulla Problematica Dei Nitrati. 2012.

Brouwer, C., Heibloem, M., 1986. Irrigation water management: irrigation water needs. Train. Man. 3.

Bucchignani, E., Montesarchio, M., Zollo, A.L., Mercogliano, P., 2016. High-resolution climate simulations with COSMO-CLM over Italy: performance evaluation and climate projections for the 21st century. Int. J. Climatol. 36, 735–756.

Carpani, M., Giupponi, C., 2010. Construction of a Bayesian Network for the Assessment of Agri-Environmental Measures–The Case Study of the Venice Lagoon Watershed. Ital. J. Agron. 5, 265–274.

Cattaneo, L., Zollo, A.L., Bucchignani, E., Montesarchio, M., Manzi, M.P., Mercogliano, P., 2012. Assessment of cosmo-clm performances over mediterranean area.

Haylock, M.R., Hofstra, N., Tank, A.M.G.K., Klok, E.J., Jones, P.D., New, M., 2008. A European daily high-resolution gridded data set of surface temperature and precipitation for 1950–2006. J. Geophys. Res. Atmos. 113.

Isotta, F.A., Frei, C., Weilguni, V., Perčec Tadić, M., Lassegues, P., Rudolf, B., Pavan, V., Cacciamani, C., Antolini, G., Ratto, S.M., 2014. The climate of daily precipitation in the Alps: development and analysis of a high-resolution grid dataset from pan-Alpine rain-gauge data. Int. J. Climatol. 34, 1657–1675.

Regione Veneto, 2014. Disciplinari Di Produzione Integrata (Tecniche Agronomiche).